須と考えられている。そこで Bay65-1942 が in vitro で mATL 細胞にアポトーシスを誘導しうるかを検討した（Fig 1）。その結果アポトーシスの指標となるゲノム DNA の断片化（Fig.1a）および TUNNEL 染色陽性細胞の出現（Fig.1b）が Bay65-1942 の存在下で認められた。またこれらの変化は Bay65-1942 の濃度依存的に増加することも観察された。

2、in vivo での生存期間延長

Bay65-1942 の in vivo での効果を検討するため、mATL 細胞を NOD-SCID マウスに移植後、Bay65-1942 を投与してその効果を観察した（Fig.2,3,4）。mATL 細胞移植翌日から薬剤投与を開始し、31 日目まで体重をモニターしつつ継続投与した。コントロールの DMSO 投与群は移植後 28 日から 32 日の間（平均 30.5 日）に全 6 頭が白血病を発症し死亡した。一方 Bay65-1942 を 800ug 投与した群の平均生存期間は 37 日であった。Kaplan-Meier 法にてそれぞれの群間で生存率の比較を行ったところ、800ug 投与群と DMSO 群および 800ug 投与群と 200ug 投与群の間で有意差がみられ、800ug 投与群において有意に生存期間が延長することが認められた。（Fig. 2）。なお 800ug 投与群では連続投与により体重減少が認められたため、断続的に薬剤投与せざるを得なかった。

3、移植後 28 日目における病理組織所見

移植後 28 日目まで治療したマウスにつき、末梢血標本と病理組織標本を作製し観察を行った（Fig. 3）。DMSO 投与群では末梢血中に多数の異型細胞の出現がみられるのに対し、Bay65-1942 を 800ug 投与した群では末梢血では少量の顆粒球を認めるのみであった。脾臓は DMSO 投与群では多数の白血病細胞の浸潤により著明に腫大していたが、Bay800ug 投与群では正常マウスの臓器と大きな違いは認められなかった。肝臓や肺でも DMSO 投与群では門脈域や気管支周囲に多数の白血病細胞の浸潤がみられるのに対し、Bay800ug 投与群ではほとんど白血病細胞の浸潤は認められなかった。

4、末梢血中白血球数の推移

薬剤投与中の白血球数の推移を Fig. 4 に示す。通常 NOD-SCID マウスの血中には少数の顆粒球のみが白血球として存在するため、mATL 細胞の移植後に末梢血中に出現してきた白血球の大多数は白血病細胞と考えられる。DMSO 投与群、Bay65-1942 を 200ug 投与した群では移植後 25 日くらいより白血球数が増加するとともにマウスの死亡が観察されだした。一方、Bay65-1942 を 800ug 投与した群では、薬剤投与期間中の移植後 31 日までは白血球数が低く抑えられていたが、薬剤投与終了直後より白血球数が急速に増加し、マウスの死亡が観察されだした。

D. 考察

今回我々はマウス ATL モデルを用い、NFkB 阻害剤 Bay65-1942 の治療効果を in vitro と in vivo で検討した。In vivo では Bay65-1942 を 800ug 投与した群において、有意な生存期間の延長が認められた。400ug 投与群ではコントロール群と比較して有意差がみられなかったため、生存期間の延長のためには少なくとも 400ug より多い量で有効濃度を保持する必要があるものと考えられた。また移植細胞数を 10^6 から $5x10^5$ 個に減らした場合でも、同様の結果が得られた（データ未公表）。これらの結果から Bay65-1942 には in vivo での生存期間の延長効果があると考えられた。

薬剤投与終了直前の 28 日目のマウス全身臓器では、Bay65-1942 を 800ug 投与した個体では病理組織学的にほとんど白血病細胞が認められなかったため Bay65-1942 により白血病細胞の増殖が強く抑えられていたものと考えられた。また、Bay65-1942 を 800ug 投与した群でも薬剤を終了すると急激に白血球数が増加し、一週間ほどの経過で腫瘍死に至っていた。これらの結果から、薬剤投与中は白血病細胞の増殖が強く抑えられるものの薬剤耐性の少数の白血病細胞が存在し、薬剤終了とともにそれらが急激に増加している可能性が示唆された。

In vitro では細胞培養中の白血病細胞に Bay65-1942 を添加することでアポトーシスが誘導されることを確認した。In vivo で観察された白血病細胞の増殖抑制効果から Bay65-1942 にはアポトーシス誘導以外にも腫瘍細胞の増殖抑制等の効果がある可能性が推測されるが、マウス体内で継代した白血病細胞は in vitro では増殖が弱く、長期間の培養が困難なため in vitro での検討は現時点では実現できていない。本マウスの白血病では in vivo での腫瘍細胞をとりまく環境因子も腫瘍の増殖や存続に重要な役割を果たしている可能性が高い。

In vitro で白血病細胞のみの長期培養が困難な点、in vivo において薬剤耐性の白血病細胞集団の存在が示唆される点から、本マウスの白血病では白血病幹細胞のようなものが背景に存在することが考えられる。実際、本マウスの白血

病細胞では白血病幹細胞様の表現型を示す細胞集団が存在することが最近明らかになった（投稿中）。今回使用したBay65-1942はin vitroとin vivoで一定の治療効果を示したが、より有効な治療のためには白血病幹細胞をも標的としうる治療法の開発を検討する必要があるかもしれない。

E. 結論

マウスATLモデルを用い、NFkB阻害剤Bay65-1942の治療効果をin vitroとin vivoで検討した。Bay65-1942がマウスATL細胞にアポトーシスを誘導することをin vitroで確認した。Bay65-1942をマウスATL細胞移植後NOD-SCIDマウスにin vivoで投与すると、最大で約1.2倍の延命効果が得られた。以上のことからBayはATL治療薬の候補のひとつとなり得るものと考えられた。

F. 健康危険情報

なし。

G. 研究発表

論文発表

1) Nagata N, Iwata N, Hasegawa H, Fukushi S, Harashima A, Sato Y, Saijo M, Taguchi F, Morikawa S, Sata T. Mouse-passaged severe acute respiratory syndrome-associated coronavirus leads to lethal pulmonary edema and diffuse alveolar damage in adult but not young mice. ***Am J Pathol.*** 172: 1625-1637, 2008.

学会発表

1. 長谷川秀樹、辻隆裕、澤洋文、佐多徹太郎成人T細胞性白血病マウスモデルにおける細胞走化因子の解析　第97回日本病理学会総会2008年5月金沢
2. 川口晶、大場靖子、木村享史、伊波英克、緒方正男、辻隆裕、佐多徹太郎、澤洋文、長谷川秀樹：ヒトATL細胞及びTaxトランスジェニックマウス由来腫瘍細胞のSDF-1αに対する走化性　第56回日本ウイルス学会総会（岡山）2008年10月
3. 辻隆裕、神戸光彦、相内章、岡本尚、佐多徹太郎、長谷川秀樹：NF-kappaB阻害剤を用いたATLモデルマウス治療の試み　第56回日本ウイルス学会総会（岡山）2008年10月

H. 知的財産権の出願、登録状況

なし

厚生労働科学研究費補助金（創薬基盤推進研究事業：ヒトゲノムテーラーメード研究事業）
平成 20 年度分担研究報告書

ATL モデルマウスから単離された腫瘍細胞およびヒト ATL 細胞の浸潤機構

分担研究者：澤　洋文（北海道大学人獣共通感染症リサーチセンター　分子病態・診断部門）
研究協力者：川口　晶（北海道大学人獣共通感染症リサーチセンター　分子病態・診断部門）
大場　靖子(北海道大学人獣共通感染症リサーチセンター　分子病態・診断部門)
伊波　英克（大分大学医学部微生物学講座）
緒方　正男（大分大学医学部附属病院　血液内科）

研究要旨

リンパ球特異的に転写を活性化する *lck* promoter 依存性に、HTLV-I の転写活性化因子である Tax 遺伝子を発現するトランスジェニックマウスから単離した腫瘍細胞および、ATL 症例から単離した腫瘍細胞を用いて、腫瘍細胞の組織への浸潤機構を解明するために、ケモカインに対する腫瘍細胞の走化性に着眼し in vitro における解析を行った。その結果、腫瘍細胞の走化性には SDF-1α-CXCR4 と MEK-ERK シグナル経路が関与することが明らかになった。さらに CXCR4 の拮抗剤である AMD3100 を用いて腫瘍細胞の走化性の抑制効果について検討を加えた。その結果 AMD3100 はマウス由来の腫瘍細胞および ATL 症例から単離した腫瘍細胞で確認された SDF-1α による ERK のリン酸化および走化性を阻害した。これらの結果から AMD3100 は ATL 治療薬の候補となり得るものと考えられた。

A. 研究目的

ATL 腫瘍細胞の組織への浸潤機構を解明するために、ケモカインに対する腫瘍細胞の走化性に着眼し解析を行い、さらに薬剤を用いてその阻害を試みた。

B. 研究方法

1) 細胞の調整

HTLV-I Tax トランスジェニックマウス由来の腫瘍細胞 1×10^6 個を RPMI に懸濁し、SCID マウスの腹腔内に接種し、マウスが白血病を発症した時点で腹水及び脾臓を回収した。さらに回収した細胞を再び SCID マウスに腹腔内接種で継代し、これを繰り返す事により増殖性を有する腫瘍細胞を濃縮した。さらに Lymphoprep kit を用いて腫瘍細胞を分離し、得られた集団を primary murine lymphoblastoid cell (pML 細胞)として実験に用いた。pML 細胞の培養は 10% Fetal Bovine Serum (FBS)を加えた RPMI 1640 medium で行なった。

臨床的に ATL の診断がなされた症例からの腫瘍細胞は Ficoll-Hypaque 比重遠心法にて分離を行い、実験を行うまで-80 ℃ で保存した。細胞融解後、15%の FBS および 1 ng/mL の最終濃度で IL-2 を加えた RPMI 1640 medium で行なった。

2) 走化性アッセイ

24 well プレートと 3 μm pore size ケモタキスチャンバーを用いて行った。細胞を 2.5×10^7 cells/ml の濃度で RPMI 1640 (0.5% bovine albumin, sodium Biocarbonae, Glutamin)に懸濁した。200 μl の細胞溶液を上部チャンバーに入れ、各濃度のケモカインを含む培地 500 μl を下部チャンバーに入れた。37℃ 5% CO_2 インキュベーターで 2 時間培養を行い、下部の培地中に移動した細胞数をカウントした。SDF-1α による刺激を確認するために pML cell (1×10^7)を 1 ml の血清を含まない RPMI 1640 培地に懸濁し、37℃で 2 時間培養した。その後 100 ng/ml の SDF-1α で刺激を加え経時的に解析した。

3) Immunoblotting

細胞を Lysis Buffer (150 mM NaCl, 2 mM EDTA, 100 mM NaF, 400 μM Na_3VO_4, 1% NP-40, complete)で溶解し、氷上に 15 分以上置いた。その後 1,000 × g、10 分、4℃で遠心後上清を回収しサンプルとした。2 × sample buffer と混合し、95℃で 5 分間ボイルしたサンプルを 10% SDS-PAGE にて分離しタンパクを PDVF membrane へ転写後抗リン酸化 ERK1/2 抗体と反応させた。次に抗 rabbit IgG 抗体を二次抗体として用いた。更に ECL-plus detection system を用いて、得られた signal は Fujifilm ルミノイメージアナライザー LAS-1000 plus を用いて検出した。

4) Flowcytometry による解析

pML 細胞の CXCR4 受容体の細胞表面での発現を調べるために、pML cell 抗 mouse-CD184/CXCR4 monoclonal antibody もしく

は陰性対照として PE-anti-Rat IgG2b を isotype control として用いて染色した。解析は FACS Canto を用いて行った。

（倫理面への配慮）

本研究計画は北海道大学遺伝子組換え実験等安全委員会にて承認されている [承認番号 20(22)]。また ATL 症例由来の腫瘍細胞を用いた実験は大分大学医学部倫理委員会で承認されている (承認番号 238)。

C. 研究結果

1) 腫瘍細胞での SDF-1α に対する走化性の亢進と細胞内シグナル伝達の解析

種々のケモカインに対する走化性の検討の結果、pML 細胞は SDF-1α に反応して、強い走化性を示した (図 1)。

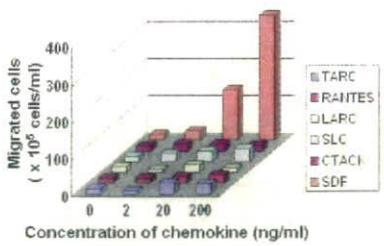

図 1 : pML 細胞の各ケモカインに対する走化性

pML 細胞は SDF-1α のレセプターである CXCR4 を表面に発現しており、CXCR4 は SDF-1α の刺激により downregulation した。pML 細胞では SDF-1α の刺激により ERK1/2 のリン酸化が増強することを見出した。

また ATL 症例から単離した腫瘍細胞でも pML 細胞と同様に、SDF-1α に反応して、ERK1/2 のリン酸化が増強に伴い強い走化性を示した。

2) AMD3100 の腫瘍細胞の走化性に対する阻害効果

AMD3100 は SDF-1α の刺激下での pML 細胞の ERK1/2 のリン酸化および走化性を濃度依存性に抑制した (図 2)。さらに ATL 症例から単離した腫瘍細胞でも同様の実験を行い、SDF-1α の刺激下 (1.25 および 12.5 μg/ml)での腫瘍細胞の ERK1/2 のリン酸化また走化性を抑制することが明らかになった (図 3)。

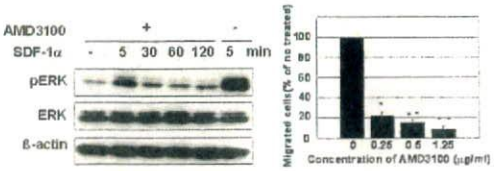

図 2: AMD3100 の pML 細胞に対する SDF-1α による ERK のリン酸化のおよび走化性に対する阻害効果

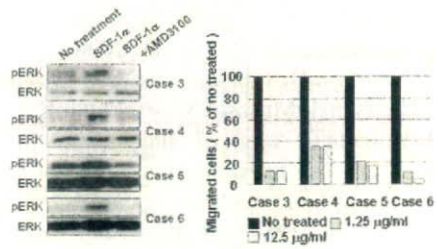

図 3 : AMD3100 の ATL 症例由来腫瘍細胞に対する SDF-1α による ERK のリン酸化のおよび走化性に対する阻害効果

D. 考察

ATL は T 細胞性の悪性腫瘍であり、HTLV-I 感染者の内 1～5%程度が感染から 40~50 年後に発症する。本疾患では多臓器への腫瘍細胞の著しい浸潤が認められ、消化器症状、皮膚症状、リンパ節腫脹などの症状を示す。その為、腫瘍細胞の浸潤のメカニズムを解明し、抑制することが ATL の治療において重要である。

本研究ではヒト ATL 症例由来腫瘍細胞および HTLV-I の転写活性化因子である Tax 遺伝子を発現するトランスジェニックマウスから単離した腫瘍細胞のいずれの細胞においても、それらの走化性に SDF-1α-CXCR4 経路が関与すること、CXCR4 を介したシグナル伝達経路である MEK-ERK が重要であることを明らかにした。

また、CXCR4 の拮抗剤である AMD3100 により ERK のリン酸化の抑制を伴って、腫瘍細胞の走化性が抑制される事が明らかとなった。SDF-1α に対する腫瘍細胞の走化性を抑制する AMD3100 は未だ治療法が確立されていない ATL の新しい治療法の候補となることが期待される。

E. 結論

ヒト ATL 症例由来腫瘍細胞および HTLV-I の転写活性化因子である Tax 遺伝子を発現するトランスジェニックマウスから単離した腫瘍細胞の走化性には SDF-1α-CXCR4 と MEK-ERK シグナル経路が関与しており、CXCR4 の拮抗剤である AMD3100 により ERK のリン酸化の抑制を伴って、腫瘍細胞の走化性が抑制された。このこ

とから AMD3100 は ATL 治療薬の候補となり得るものと考えられた。

F. 健康危険情報

なし。

G. 研究発表

1. 論文発表

1) Orba Y, Sunden Y, Suzuki T, Nagashima K, Kimura T, Tanaka S, Sawa H. Pharmacological cdk inhibitor R-Roscovitine suppresses JC virus proliferation. ***Virology*** 370: 173-183, 2008

2) Ohnishi N, Yuasa H, Tanaka S, Sawa H, Miura M, Matsui A, Higashi H, Musashi M, Iwabuchi K, Suzuki M, Yamada G, Azuma T, Hatakeyama M. Transgenic expression of Helicobacter pylori CagA induces gastrointestinal and hematopoietic neoplasms in mouse. ***Proc Natl Acad Sci USA*** 105: 1003-1008, 2008

3) Hirano M, Rakwal R, Shibato J, Sawa H, Nagashima K, Ogawa Y, Yoshida Y, Iwahashi H, Niki E, Masuo Y. Proteomics- and transcriptomics-based screening of differentially expressed proteins and genes in brain of Wig rat: A model for attention deficit hyperactivity disorder (ADHD) research. ***J Proteome Res***. 7:2471-2489, 2008

2. 学会発表

1) 長谷川 秀樹、辻 隆裕、澤 洋文、佐多 徹太郎:成人 T 細胞性白血病マウスモデルにおける細胞走化因子の解析。第 97 回日本病理学会総会 2008 年、5 月、金沢

2) 大西 なおみ、湯浅 眸、田中 伸哉、澤 洋文、三浦 太浩、松井 敦史、東 秀明、岩淵 和也、武蔵 学、鈴木 操、山田 源、東 健、畠山 昌則:ヘリコバクター・ピロリ cagA 遺伝子導入マウスにおける消化管腫瘍ならびに血液系腫瘍の発生。日本分子生物学会第 8 回春季シンポジウム、2008 年 5 月 25-27 日、札幌

3) 川口 晶、大場 靖子、木村 享史、伊波 英克、緒方 正男、佐多 徹太郎、澤 洋文、長谷川 秀樹:ATL 腫瘍細胞の走化性における CXCR4 を介したシグナル経路の解析。第 73 回日本インターフェロン・サイトカイン学会学術集会・第 19 回日本生体防御学会学術総会・第 45 回補体シンポジウム 合同大会、2008 年 7 月 10-12 日、北海道大学学術交流会館、札幌

4) 川口 晶、大場 靖子、木村 享史、伊波 英克、緒方 正男、辻 隆裕、佐多 徹太郎、澤 洋文、長谷川 秀樹:HTLV-I Tax トランスジェニックマウス由来腫瘍細胞の SDF-1α に対する走化性とその阻害。第 1 回 HTLV-1研究会・合同班会議、2008 年 8 月 23-24 日、東京大学医科学研究所、東京

5) 川口 晶、大場 靖子、木村 享史、伊波 英克、緒方 正男、辻 隆裕、佐多 徹太郎、澤 洋文、長谷川 秀樹:ヒトATL細胞及びTaxトランスジェニックマウス由来腫瘍細胞のSDF-1αに対する走化性とその阻害。第56回日本ウイルス学会総会、2008年10月26-28日、岡山コンベンションセンター、岡山

6) 大場 靖子、鈴木 忠樹、木村 享史、澤 洋文: ヒトポリオーマウイルスJCVのLarge T Antigenによる G2チェックポイント活性化機構。第56回日本ウイルス学会総会、2008年10月26-28日、岡山コンベンションセンター、岡山

7) 大西 なおみ、田中 伸哉、澤 洋文、三浦 太浩、東 秀明、東 健、畠山 昌則:ヘリコバクター・ピロリ cagA 遺伝子導入マウスにおける消化管腫瘍ならびに血液系腫瘍の発生。第 67 回日本癌学会学術総会、2008 年 10 月 28-30 日、名古屋国際会議場、名古屋

8) 大場 靖子、鈴木 忠樹、木村 享史、澤 洋文:JC ウイルス large T antigen による G2/M check point 活性化機構の解析。第 31 回日本分子生物学会年会、第 81 回日本生化学会大会 2008 年 12 月 9-12 日、神戸

H. 知的財産権の出願・登録状況(予定を含む。)

1. 特許出願: なし
2. 実用新案登録:なし
3. その他 :なし

Ⅲ. 研究成果の刊行に関する一覧表

雑誌

発表者氏名	論文タイトル名	発表誌名	巻号	ページ	出版年
Saitohら	Overexpressed NF- κB inducing kinase contributes to the tumorigenesis of adult T-cell leukemia and Hodgkin Reed-Sternberg cells	***Blood***	111	5118-5129	2008
Miyakeら	Induction of apoptosis in Epstein-Barrvirus-infecte B-lymphocytes by the NF-κB inhibitor DHMEQ	***Microbes Infect***	10	748-756	2008
Watanabeら	Identification of the Rela domain responsible for action of a new NFkappaB inhibitor DHMEQ	***Biochem Biophys Res Commun***	376	310-314	2008
Shimizuら.	Impaired Tax-specific T-cell responses with insufficient control of HTLV-1 in a subgroup of individuals	***Cancer Sci***	100	481-489	2008
Uchimaruら	Factors predisposing to HTLV-1 infection in residents of the greater Tokyo area	***Int J Hematol***	88	565-570	2008
Tsukasakiら	Definition, Prognostic Factors, Treatment and Response Criteria of Adult T-cell Leukemia-Lymphoma: A Proposal from an International Consensus Meeting	***J Clin Oncol***	27	453-459	2009
Kawaseら	Identification of human minor histocompatibility antigens based on genetic association with highly parallel genotyping of pooled DNA.	***Blood.***	111	3286-3294	2008
Akagiら	Frequent genomic abnormalities in acute myeloid leukemia/myelodysplastic syndrome with normal karyotype.	***Haematologica***	94	213-223.	2008
Chenら	Oncogenic mutations of ALK kinase in neuroblastoma.	***Nature***	455	971-974	2008
Walshら	ERCC5 is a novel biomarker of ovarian cancer prognosis	***J Clin Oncol.***	26	2952-2958	2008
Kawamataら	Cloning of genes involved in chromosomal translocations by high-resolution single nucleotide polymorphism genomic microarray.	***Proc Natl Acad Sc***	105	11921-11926	2008
Hamaguchiら	Application of quantitative gene expression analysis for pertussis vaccine safety control.	***Vaccine***	26	4686-4696	2008
Otsuboら	Current risks in blood transfusion in Japan.	***Jpn J Infect Dis.***	61	427-433	2008
Nagataら	Mouse-passaged severe acute respiratory syndrome-associated coronavirus leads to lethal pulmonary edema and diffuse alveolar damage in adult but not young mice	***Am J Pathol***	172	1625-1637	2008
Orbaら	Pharmacological cdk inhibitor R-Roscovitine suppresses JC virus proliferation	***Virology***	370	173-183	2008
Ohnishiら	Transgenic expression of Helicobacter pylori CagA induces gastrointestinal and hematopoietic neoplasms in mouse	***Proc Natl Acad Sci USA***	105	1003-1008	2008
Hiranoら	Proteomics- and transcriptomics-based screening of differentially expressed proteins and genes in brain of Wig rat: A model for attention deficit hyperactivity disorder (ADHD) research	***J Proteome Res***	7	2471-2489	2008

Overexpressed NF-κB–inducing kinase contributes to the tumorigenesis of adult T-cell leukemia and Hodgkin Reed-Sternberg cells

Yasunori Saitoh,[1] Norio Yamamoto,[1] M. Zahidunnabi Dewan,[1] Haruyo Sugimoto,[1] Vicente J. Martinez Bruyn,[1] Yuki Iwasaki,[1] Katsuyoshi Matsubara,[1] Xiaohua Qi,[1] Tatsuya Saitoh,[2] Issei Imoto,[3] Johji Inazawa,[3] Atae Utsunomiya,[4] Toshiki Watanabe,[5] Takao Masuda,[6] Naoki Yamamoto,[1,7] and Shoji Yamaoka[1]

[1]Department of Molecular Virology, Graduate School of Medicine, Tokyo Medical and Dental University, Tokyo; [2]Department of Host Defense, Research Institute for Microbial Diseases, Osaka University, Suita; [3]Department of Molecular Cytogenetics, Medical Research Institute and School of Biomedical Science, Tokyo Medical and Dental University, Tokyo; [4]Department of Hematology, Imamura Bun-in Hospital, Kagoshima; [5]Department of Medical Genome Sciences, Graduate School of Frontier Sciences, University of Tokyo, Tokyo; [6]Department of Immunotherapeutics, Graduate School of Medicine, Tokyo Medical and Dental University, Tokyo; and [7]AIDS Research Center, National Institute of Infectious Diseases, Tokyo, Japan

The nuclear factor-κB (NF-κB) transcription factors play important roles in cancer development by preventing apoptosis and facilitating the tumor cell growth. However, the precise mechanisms by which NF-κB is constitutively activated in specific cancer cells remain largely unknown. In our current study, we now report that NF-κB–inducing kinase (NIK) is overexpressed at the pretranslational level in adult T-cell leukemia (ATL) and Hodgkin Reed-Sternberg cells (H-RS) that do not express viral regulatory proteins. The overexpression of NIK causes cell transformation in rat fibroblasts, which is abolished by a super-repressor form of IκBα. Notably, depletion of NIK in ATL cells by RNA interference reduces the DNA-binding activity of NF-κB and NF-κB–dependent transcriptional activity, and efficiently suppresses tumor growth in NOD/SCID/γc^{null} mice. These results indicate that the deregulated expression of NIK plays a critical role in constitutive NF-κB activation in ATL and H-RS cells, and suggest also that NIK is an attractive molecular target for cancer therapy. (Blood. 2008;111:5118-5129)

Introduction

The nuclear factor-κB (NF-κB) transcription factors are known to regulate the expression of a wide range of genes involved in development, immune responses, apoptosis, and carcinogenesis as dimers of the REL family members, RelA, RelB, c-Rel, p50, and p52.[1] The p50 and p52 proteins are generated by proteasome-mediated processing of their precursors, p105 and p100, respectively. In resting cells, Rel proteins are sequestered in the cytoplasm through their interactions with the ankyrin repeats of the inhibitory proteins IκBα, -β, and -ϵ, as well as the precursor proteins p105 and p100. On stimulation, signals converge at the multiprotein IκB kinase (IKK) complex, which is composed of 2 catalytic subunits, IKK1/α and IKK2/β, and the scaffolding proteins, NF-κB essential modulator (NEMO, also known as IKKγ) and ELKS.[2] Phosphorylation by the IKK complex of specific serine residues on the IκB or precursor proteins results in their poly-ubiquitination and proteasome-dependent degradation or processing.[2] Released NF-κB then translocates to the nucleus and regulates expression of target genes.

NF-κB signaling pathways are largely classified as either canonical or noncanonical based on the stimuli and targets of the IKK complex.[2] Canonical activation is induced by stimuli, such as tumor necrosis factor-α (TNFα) and interleukin-1β, and involves NEMO- and IKK2/β-dependent phosphorylation and the subsequent degradation of IκB proteins. Noncanonical NF-κB pathways are activated after the stimulation of a range of TNF receptor family members, such as B-cell activating factor belonging to the TNF family (BAFF) receptor, lymphotoxin-β receptor, Fn14 and CD40, and direct NF-κB–inducing kinase (NIK)- and IKK1/α-dependent phosphorylation and subsequent processing of p100, leading to activation of NF-κB complexes containing RelB.[2,3] Of note in this context, the noncanonical pathways operate in a delayed fashion and are sensitive to protein synthesis inhibition.[4,5]

Compared with the mechanisms underlying the transduction of ligand-induced signaling to NF-κB activation, much less is known about how NF-κB is constitutively activated in a variety of cancer cells.[6] Constitutively high NF-κB activity has typically been demonstrated in human hematopoietic cancer cells, including adult T-cell leukemia (ATL), Hodgkin lymphoma, and multiple myeloma cells.[7,8] We have previously reported the aberrant expression of p52 in ATL and Hodgkin Reed-Sternberg (H-RS) cells that do not express viral regulatory proteins, such as Tax of the human T-cell leukemia virus or latent membrane protein 1 of the Epstein-Barr virus.[9,10] In addition, IKK activation in ATL and H-RS cells was found to be sensitive to protein synthesis inhibition.[10,11] These results indicate that the noncanonical pathways of NF-κB activation operate in these cancer cells. Aberrant p52 expression has also been reported in other types of cancer cells, including breast,[12] prostate,[13] pancreas,[14] and colon.[15] However, the actual triggers of noncanonical NF-κB activation in these cancer cells remain largely unknown except for certain multiple myeloma cells that have mutations in the *NIK*, *TRAF3*, and related genes.[16,17]

Submitted September 10, 2007; accepted February 17, 2008. Prepublished online as *Blood* First Edition paper, February 27, 2008; DOI 10.1182/blood-2007-09-110635.

The online version of this article contains a data supplement.

The publication costs of this article were defrayed in part by page charge payment. Therefore, and solely to indicate this fact, this article is hereby marked "advertisement" in accordance with 18 USC section 1734.

NIK is a serine-threonine kinase that is an essential participant in the induction of the IKK1-dependent processing of p100 as well as IκB degradation in response to stimuli, such as CD70, CD40 ligand, and BAFF.[18] It has also been reported previously that the IKK complex is recruited to CD27 in a manner dependent on NIK function. However, the mechanism by which NIK activity is regulated thereafter was unknown until it was recently demonstrated that these stimuli protect basally translated endogenous NIK protein from proteasome-mediated degradation.[19,20] Liao et al reported that the interaction of NIK with TNF receptor–associated factor 3 (TRAF3) is responsible for the rapid degradation of NIK and that noncanonical NF-κB stimuli induce the degradation of TRAF3 and the elevation of NIK expression.[19] In a separate study, Qing et al have demonstrated that noncanonical NF-κB stimuli stabilize the NIK protein but do not modify its RNA expression or protein translation.[20] The findings of these studies explain the delay in triggering the noncanonical pathway and its high sensitivity to protein synthesis inhibition.

Because NIK is a central regulator of the noncanonical pathway of NF-κB activation, we have investigated in our current study how this kinase is regulated in hematopoietic cancer cells, in which IKK is constitutively activated in the absence of viral regulators.

Methods

Cell culture

ED40515(−),[21] ATL-43Tb(−),[22] and TL-Om1[23] are human T-cell leukemia virus type-I (HTLV-I)–infected T-cell lines established from the leukemic cells of ATL patients. The H-RS cell lines, HDLM-2, L428, and L540, were purchased from the German Collection of Micro-organisms and Cell Cultures (Braunschweig, Germany). CEM[24] and Jurkat[25] are HTLV-I–free human T-lymphoblastic leukemia cell lines. A human B-cell line, Romas RG69,[20] was a kind gift from Dr Gutian Xiao (State University of New Jersey, Piscataway, NJ). Primary leukemia cells derived from ATL patients were obtained under informed consent at Imamura Bun-in Hospital and supplied through the Joint Study on Predisposing Factors of ATL Development. The patients were diagnosed with ATL on the basis of clinical and hematologic features and the presence of antibodies to ATL-associated antigens in serum and of the HTLV-I proviral genome in the leukemia cells. Use of peripheral blood lymphocytes from ATL patients for research purposes was approved by the institutional review board of each institute. Peripheral blood mononuclear cells (PBMCs) derived from healthy donors were also obtained under informed consent. PBMCs were isolated from both ATL patients and healthy donors by density gradient separation with Ficoll-Plaque PLUS (Amersham Biosciences, Uppsala, Sweden). Cells were maintained in RPMI 1640 supplemented with 10% fetal bovine serum, 100 U/mL penicillin G, and 100 μg/mL streptomycin sulfate; 5R is a NEMO-deficient subline of the Rat-1 cell line and has been described previously.[26] B5 and h12 are sublines of Rat-1 and 5R, respectively, express the blasticidin deaminase gene under the control of an NF-κB–dependent promoter, and have also been described previously.[26,27] Plat-E packaging cells were described previously.[28] B5, h12, Plat-E, 293T cells, and mouse embryonic fibroblasts were maintained in Dulbecco modified Eagle medium supplemented with 10% fetal bovine serum, 100 U/mL penicillin G, and 100 μg/mL streptomycin sulfate. Anchorage-independent cell growth was examined essentially as described previously.[29] Images were captured using an inverted microscope (IX70, Olympus, Tokyo, Japan) and processed with Openlab 3.0.2 software (Improvision, Coventry, United Kingdom). Cells used in this study were all maintained at 37°C in air containing 5% CO_2.

Virus infection and transfection

Plat-E cells were transfected with pMRX-HA-NIK-ires-puro, pMRX-HA-kd-NIK-ires-puro, or pMRX-HA-ires-puro (EV1) (Document S1, available on the *Blood* website; see the Supplemental Materials link at the top of the online article) using the calcium phosphate precipitation method. Culture supernatants were collected 48 hours after transfection and filtered. B5 and h12 cells were infected for 2 hours in the presence of 10 μg/mL polybrene. Infected cells were then cultured in medium containing 2 μg/mL puromycin, and cell clones were isolated. Rat fibroblasts expressing SR-IκBα or its empty control vector (EV2) were established essentially as described previously.[10] For production of lentiviruses, 293T cells were cotransfected with pCS-puro-Ctli, pCS-puro-NIKi-1, or pCS-puro-NIKi-2 (Document S1) together with the pCMVΔR8.2 packaging construct and pHCMV-VSV-G (kind gifts from Dr I.S.Y. Chen) using FuGENE 6 (Roche Applied Science, Indianapolis, IN). Culture supernatants were collected 48 hours after transfection and filtered. ED40515(−) and ATL-43Tb(−) cells were infected once or twice with 24 hours interval with these lentiviruses for 6 hours in the presence of 10 μg/mL polybrene. At 48 hours after the infection, cells were cultured in medium containing 2 μg/mL puromycin for an additional 48 hours. These infectants were subjected to immunoblotting, electrophoretic mobility shift assay (EMSA), and transient transfection with 2 μg of IgκCona-luc[30] and pEF1-LacZ[26] using DMRIE-C (Invitrogen, Carlsbad, CA) according to the manufacturer's instructions. Assays for luciferase and β-galactosidase were performed 48 hours after transfection by standard methods. Luciferase activity was normalized on the basis of β-galactosidase activity. The growth of lentivirus-infected cells was determined by the trypan blue staining method.

Immunoprecipitation

For the immunoprecipitation of endogenous NIK, approximately 2×10^7 cells were lysed in buffer A (20 mM Tris-HCl, pH7.5, 0.5% Nonidet P-40, 150 mM NaCl supplemented with 1 μg/mL aprotinin, 1 μg/mL leupeptin, 0.57 mM phenylmethanesulphonylfluoride, 10 μM MG132, 10 μM MG115) followed by preclearing with purified rabbit IgG (Cedarlane Laboratories, Hornby, ON) and protein G-Sepharose beads (Pierce Biotechnology, Rockford, IL). After centrifugation at 14000 rpm for 3 minutes, supernatants were subjected to immunoprecipitation with purified nonimmune rabbit IgG or anti-NIK antibody (#4994) (Cell Signaling Technology, Danvers, MA). Immunoprecipitates were washed 3 times with TNT buffer (20 mM Tris-HCl, pH 7.5, 200 mM NaCl, and 1% Triton X-100). Endogenous NIK proteins were detected by immunoblotting with anti-NIK antibody (#4994). For the immunoprecipitation of HA-tagged NIK, 750 μg cell lysates prepared with buffer A was subjected to immunoprecipitation with anti-HA antibody (12CA5, a kind gift from Dr A. Israël, Institut Pasteur Paris, Paris, France). Immunoprecipitates were washed 3 times with TNT buffer. HA-tagged NIK proteins were detected by immunoblotting with anti-NIK antibody. For immunoprecipitation of endogenous IKK1/2, 1500 μg cell lysates prepared with buffer A were subjected to immunoprecipitation with anti-IKK1 monoclonal antibody (B78-1; BD PharMingen, San Diego, CA) or purified mouse IgG2b (MI10-104; Bethyl Laboratories, Montgomery, TX). Immunoprecipitates were washed 3 times with TNT buffer. Expression of endogenous proteins was detected by immunoblotting with antiphospho-IKK1/IKK2 (Ser180/Ser181) (#2681; Cell Signaling Technology), anti-IKK1 (H-744), or anti-IKK2 (H-470; Santa Cruz Biotechnology, Santa Cruz, CA) antibodies.

Quantitative RT-PCR

Total RNA was extracted using Isogen reagents (Nippon Gene, Tokyo, Japan) according to the manufacturer's instructions. Quantitative RT-PCR amplifications were performed with 100 ng total RNA, 0.3 μM of each primer, and 0.25 μM TaqMan probe using an ABI-7700 Sequence Detector (Applied Biosystems, Foster City, CA): reverse transcription was performed at 48°C for 30 minutes, Taq DNA polymerase was activated at 95°C for 10 minutes, followed by 45 amplification cycles of 95°C for 15 seconds, and annealing and extension at 60°C for 1 minute. The *NIK*, *VEGF*, *ICAM-1*, and *MMP-9* mRNA levels were normalized based on the amount of *18S* ribosomal RNA determined simultaneously by the real-time RT-PCR.

Mice and inoculation of cells

NOD/SCID/γc^{null} (NOG)[31] mice were purchased from the Central Institute for Experimental Animals (Kawasaki, Japan). All mice were maintained under specific pathogen-free conditions in the Animal Center of Tokyo Medical and Dental University (Tokyo, Japan). The Ethical Review Committee of the institute approved the experimental protocol. ED40515(−) cells expressing Ctli or NIKi-1 and -2 were washed twice with serum-free RPMI 1640 and resuspended in the same medium. Mice were anesthetized with ether and inoculated subcutaneously in the postauricular region with 5×10^6 cells per mouse, as described previously.[31] We measured tumor size and weight 2 weeks after cell inoculation.

Statistics

Statistical significance was evaluated using a 2-tailed, unpaired Student's *t* test. *P* values less than .05 were considered to be significant.

Results

NIK is aberrantly expressed in both adult T-cell leukemia and Hodgkin Reed-Sternberg cells

The constitutive processing of p100 to p52 in ATL and H-RS cells[9,10] prompted us to examine whether NIK is aberrantly expressed in both established and primary ATL cells. Immunoblotting of whole-cell lysates prepared from ATL or H-RS cells did not show any detectable NIK signal (data not shown); however, when endogenous NIK was immunoprecipitated from approximately 20 million of these cells and subjected to immunoblotting, NIK was specifically detectable in anti-NIK immunoprecipitates from ATL and H-RS cells, but not from control cells, such as CEM and Jurkat (Figure 1A). Previous studies revealed that inhibition of the proteasome function allowed for detection of endogenous NIK in simple whole-cell lysates of B-cell lines.[19,20] Treatment of ED-40515(−) cells with the MG132 proteasome inhibitor for 3 hours before harvesting enabled us to observe robust endogenous NIK expression at the expected position (Figure 1B). Lysates of 293T cells with or without exogenous NIK expression were used as the positive and negative controls, respectively. We next examined the NIK expression levels as well as those of p100 phosphorylated at serine residues 866 and 870 in a panel of ATL, H-RS, and control cells (Figure 1C). No appreciable NIK expression could be observed in control CEM and Jurkat T-cell lines treated with MG132, in which NF-κB is not constitutively activated. Proteasome inhibition induced strong NIK expression in other Tax-negative ATL-derived cell lines, ATL-43Tb(−) and TL-Om1. Proteasome inhibition also strongly augmented NIK expression in H-RS cells, but only weakly so in the control B-cell lines, RG69. These results indicate that the steady-state levels of NIK of the authentic size are elevated in ATL and H-RS cells, and suggest that NIK may be abundantly produced in ATL and H-RS cells, but is rapidly degraded by the proteasome. The levels of NIK expression correlated well with those of phosphorylated p100 (Figure 1C). Moreover, p52 and the phoshorylated form of IκBα were also abundant in ATL and H-RS cell lines, but not in the control T-cell lines (Figure 1C). These results indicate that the overexpression of NIK is closely linked to the downstream events leading to constitutive activation of the canonical and noncanonical NF-κB pathways in ATL and H-RS cells. A previous study suggested that L428 cells express a C-terminally truncated form of IκBα and that the phosphorylated form of this protein was accumulated after treatment of the cells with proteasome inhibitor or dexamethasone.[32,33] In agreement with this, we did not detect IκBα expression with the antibody used in this study, which recognizes the C-terminus of the protein, but detected the phoshorylated form of this IκBα only after treatment with MG132 (data not shown).

We next investigated *NIK* expression at the mRNA level by quantitative PCR (Figure 1D) and found that that *NIK* transcripts were at between 20- and 100-fold higher levels in ATL and H-RS cells, compared with CEM cells. Next, actinomycin D was used to block new mRNA synthesis, so that decay of existing transcripts could be detected. Quantitative PCR analyses revealed that the half-life of *NIK* mRNA was approximately 3 hours both in the ATL and control T cells (Figure 1E). Essentially similar results were obtained with the other cell lines shown in Figure 1D, including H-RS cell lines (data not shown). A previous report has demonstrated that NF-κB is constitutively activated in primary ATL cells in the peripheral blood.[34] We therefore quantified the *NIK* mRNA levels in PBMCs from both healthy donors and ATL patients (Figure 2A), and found that *NIK* mRNA is overexpressed in PBMCs of 15 of 21 ATL patients. Actinomycin D treatment of PBMCs further revealed that *NIK* mRNA was not apparently stabilized in primary ATL cells (Figure 2B). Moreover, fluorescence in situ hybridization studies on primary ATL cells failed to detect amplification or translocation of the *NIK* gene (Figure S1; Table S2). Finally, when PBMCs were cultured for 3 hours in the presence of MG132, NIK protein was detectable in cells from an ATL patient showing abundant *NIK* mRNA expression, but not in those from a healthy donor (Figure 2C).

NIK transforms rat fibroblasts in an NF-κB–dependent manner

To further explore the roles for NIK during cell transformation, we infected the 3T3-like rat fibroblast cell line Rat-1 with a retroviral vector expressing human NIK and examined its oncogenic activity. As expected, cells transduced with this NIK vector exhibited strong NF-κB DNA binding activity within 36 hours (data not shown). Rat-1 cells transduced with a control retrovirus became resistant to the selection marker puromycin approximately 24 hours after infection and continued to proliferate rapidly. In contrast, Rat-1 cells transduced with the NIK expression vector expressed a readily detectable level of NIK, had a transformed morphology, but ceased proliferating and died within 3 to 4 days after becoming resistant to puromycin. Cells that survived 2 weeks of puromycin selection after NIK transduction eventually appeared indistinguishable from those transduced with the control vector and showed no detectable NIK expression or NF-κB DNA binding activity (data not shown).

Based on these observations, we speculate that the retroviral overexpression of NIK is toxic to the cells so that only cells that had lost its expression could emerge from the puromycin-resistant pools. To address this problem, we used B5 and h12 cells carrying an integrated Igκ2bsrH plasmid that confers resistance to the antibiotic blasticidin S when cells are constitutively expressing active NF-κB.[26] B5 cells are derived from Rat-1 cells, and h12 cells are from 5R cells that lack NEMO expression. When the B5 and h12 cells were transduced with the wild-type NIK retroviral expression vector and subjected to selection with both puromycin and blasticidin S, the majority of the resultant cell clones maintained detectable NIK expression (Figure 3A), elevated catalytic activity of IKK (Figure 4), and the initial transformed morphology (Figure 5B). On the other hand, when B5 and h12 cells were transduced with a retrovirus vector expressing a catalytically inactive mutant form of NIK and selected with puromycin alone, the cells successfully

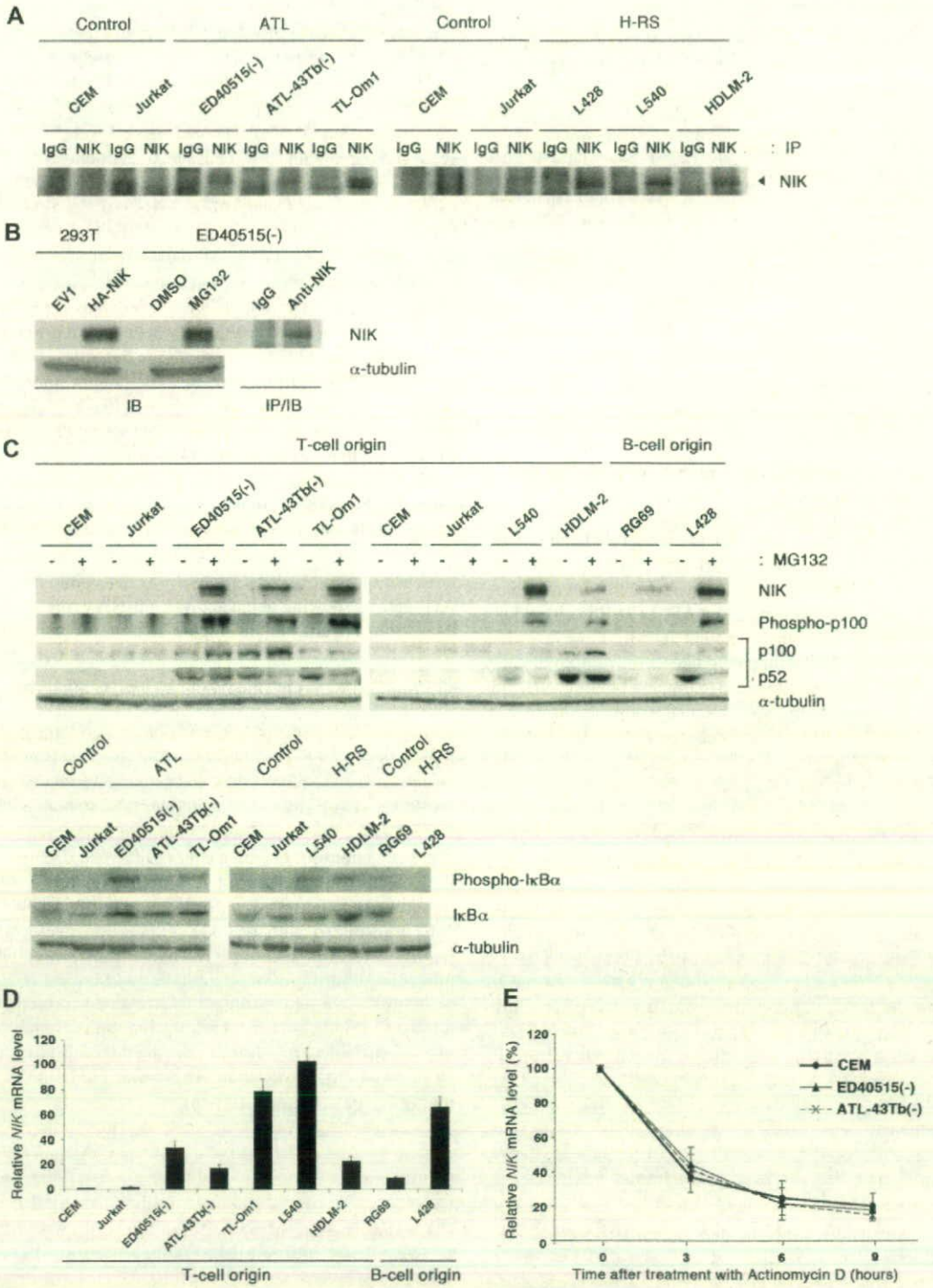

Figure 1. NIK protein is overexpressed in established ATL and Hodgkin Reed-Sternberg cells. (A) Steady-state levels of NIK expression in the ATL and H-RS cell lines were revealed by immunoprecipitation-coupled immunoblotting. Approximately 2×10^7 cells were lysed with buffer A. After preclearing, immunoprecipitation was performed at 4°C, using anti-NIK antibody (NIK) or its isotype IgG (IgG). After 3 washes with TNT buffer, immune complexes were analyzed by immunoblotting with anti-NIK antibody. (B) 293T cells were transfected with pMRX-HA-iresPuro or pMRX-HA-NIKiresPuro for 24 hours. Whole-cell lysates were used as negative and positive controls. ED40515(−) cells were pretreated with (+) or without (−) MG132 (20 μM) for 3 hours, lysed with RIPA buffer, and subjected to immunoblotting with anti-NIK or anti-α-tubulin antibodies. Immunoprecipitation-coupled immunoblotting was performed as in panel A. (C) Top panels: control T-cell lines (CEM and Jurkat), leukemic cell lines derived from ATL patients that do not express Tax (ED40515(−), ATL43-Tb(−), and TL-Om1, a control B-cell line (RG69), and H-RS cell lines (HDLM-2 and L540) were pretreated with (+) or without (−) MG132 (20 μM) for 3 hours, and 30 μg of the whole-cell extracts were subjected to Western blot analysis with the antibodies to the indicated proteins. Bottom panels: Whole-cell extracts from the indicated cell lines were analyzed by Western blotting with the antibodies to the indicated proteins. (D) Total RNA was extracted from the indicated cell lines and subjected to real-time RT-PCR to quantify the *NIK* mRNA levels. The *NIK* mRNA levels were normalized to *18S* RNA. The relative *NIK* mRNA levels shown represent the fold increases in mRNA abundance, relative to that of the CEM cells (arbitrarily set at 1). (E) Cells were cultured in the presence of actinomycin D (5 μg/mL) for the times indicated, and then total RNA was isolated and subjected to quantitative RT-PCR as in panel D. Data are expressed as mean plus or minus SD of 3 independent experiments. The relative amounts of *NIK* mRNA shown represent the percentages in mRNA abundance, relative to that of each cell line before the addition of actinomycin D (arbitrarily set at 100%). IB indicates immunoblotting; IP, immunoprecipitation.

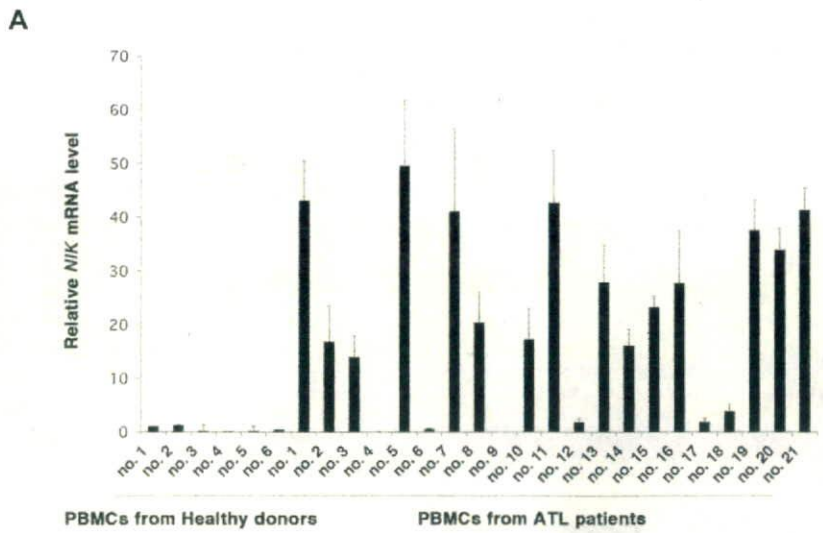

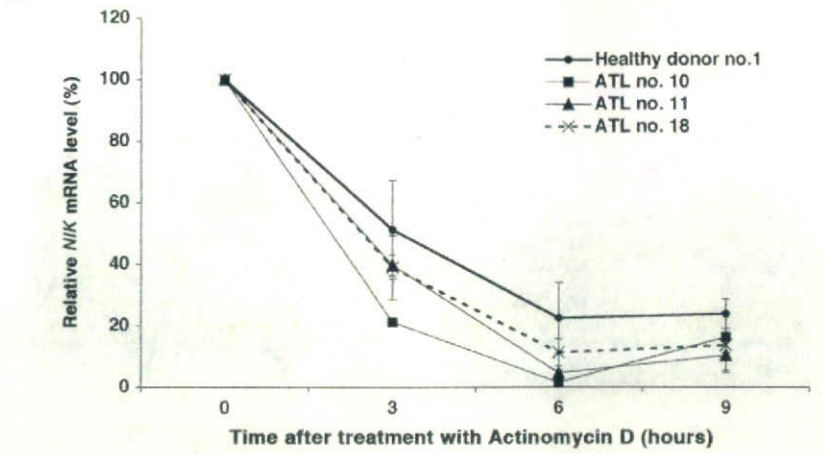

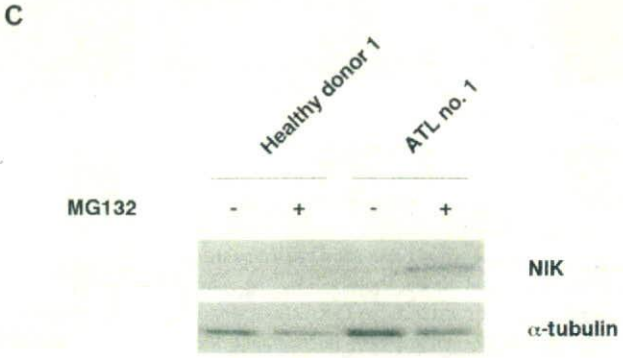

Figure 2. Overexpression of the *NIK* mRNA and protein in PBMCs from ATL patients. (A) Total RNA was extracted from PBMCs from healthy donors and ATL patients and then subjected to quantitative RT-PCR. The *NIK* mRNA levels were normalized to *18S* RNA. The relative *nik* mRNA levels shown represent the fold increases in mRNA abundance relative to that of healthy donor 1 (arbitrarily set at 1). These data are expressed as the mean plus or minus SD of 3 independent experiments. (B) PBMCs were cultured in the presence of actinomycin D (5 μg/mL) for the times indicated, and then total RNA was isolated and subjected to quantitative RT-PCR. The relative amounts of *NIK* mRNA shown represent the percentages in mRNA abundance, relative to that of PBMCs before the addition of actinomycin D (arbitrarily set at 100%). (C) PBMCs from a healthy donor and an ATL patient were treated with (+) or without (−) MG132 (20 μM) for 3 hours, lysed with RIPA buffer, and subjected to immunoblotting with anti-NIK or anti-α-tubulin antibodies.

expressed this protein (Figure 3A) without significant morphologic change (Figure 5B) or constitutive NF-κB activation (Figure 3C). As expected, these cells failed to survive selection with blasticidin S (data not shown).

The expression of wild-type NIK in B5 and h12 cells potently induces p52 expression and NF-κB DNA binding activity, whereas the catalytically inactive NIK mutant does not (Figure 3B,C). We also found a specifically phosphorylated form of IκBα in cells expressing wild-type NIK (Figure 3A). Super-shift experiments revealed that the NF-κB–DNA binding complexes in B5 and h12 cells expressing NIK involve p50, RelB, and RelA (Figure 4D). The presence of p52 in the DNA binding complexes could not be examined, however, because an antibody recognizing rat p52 in super-shift assay is not currently available. Instead, we analyzed DNA-binding complexes induced by NIK expression in wild-type mouse embryonic fibroblasts (Figure S2). Retroviral overexpression of NIK indeed induced DNA-binding NF-κB complexes containing p52, and enhanced expression of p52 and phosphorylated form of IκBα.

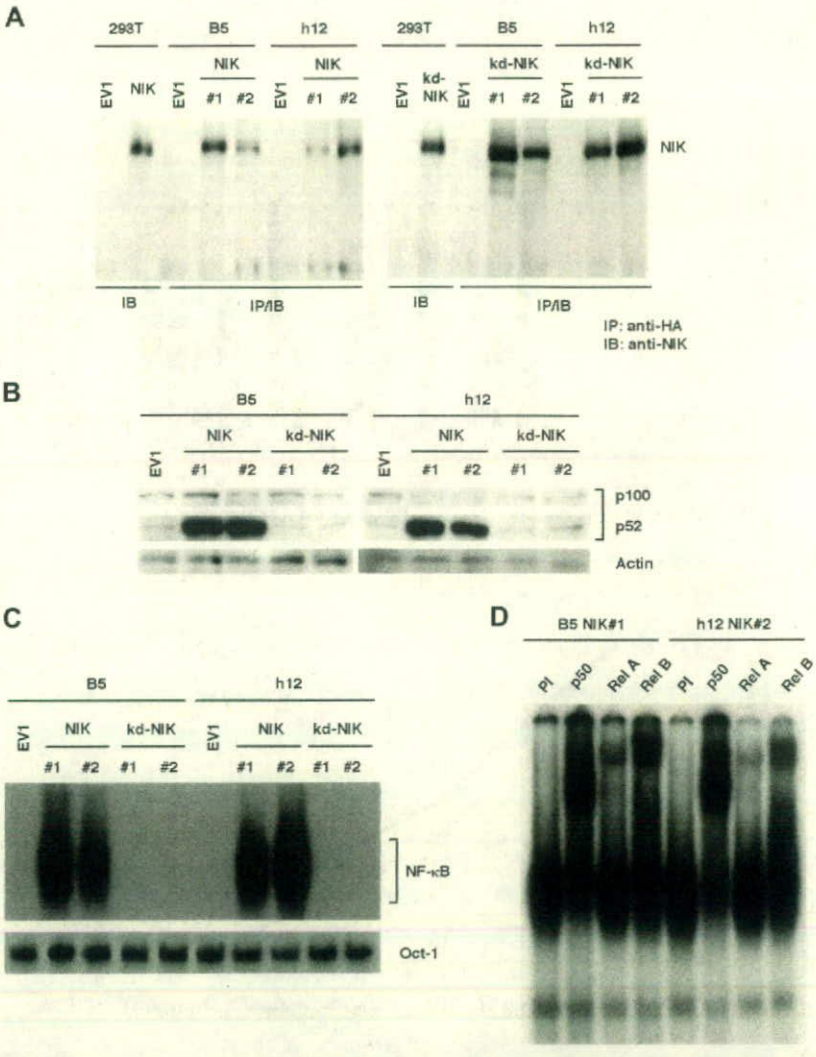

Figure 3. NIK induces constitutive NF-κB activity in rat fibroblasts. (A) B5 and h12 cells were infected with retroviruses capable of expressing HA-tagged NIK (NIK) or catalytically inactive NIK (kd-NIK). Pools of B5 and h12 cells transduced with the control pMRX-HAiresPuro vector (EV1) were used as a control. Cytoplasmic extracts from EV1 and 2 independent cell clones (no. 1 and no. 2) were subjected to immunoprecipitation using antibody against the HA epitope. Immunoprecipitates were then resolved by 8% SDS-PAGE and subjected to immunoblotting with anti-NIK antibody. 293T cells were transiently transfected with the pMRX-HAiresPuro vector (EV1) or pMRX-HA-NIKiresPuro (NIK). Cytoplasmic extracts (30 μg) were then used for immunoblotting as negative and positive controls, respectively. (B) Elevated p52 production in rat fibroblasts. Whole-cell lysates from B5 and h12 cells expressing wild-type NIK or kd-NIK were subjected to SDS-PAGE and immunoblotting with anti-p52 for detection of p100 and p52 or antiactin antibodies. (C) Elevated NF-κB–DNA binding activity in rat fibroblasts; 5 μg of nuclear extracts prepared from B5 and h12 cells expressing wild-type NIK or kd-NIK were analyzed by EMSA, using oligonucleotides encoding an NF-κB–binding sequence or Oct-1–binding sequence as probes. (D) DNA-binding NF-κB components in B5 and h12 cells expressing wild-type NIK were analyzed by super-shift EMSA. Nuclear extracts (5 μg) from B5 NIK#1 and h12 NIK#2 cells were preincubated for 30 minutes with preimmune (PI), anti-p50, anti-RelA or anti-RelB sera, and then subjected to EMSA with the NF-κB–specific probe. IB indicates immunoblotting; IP, immunoprecipitation.

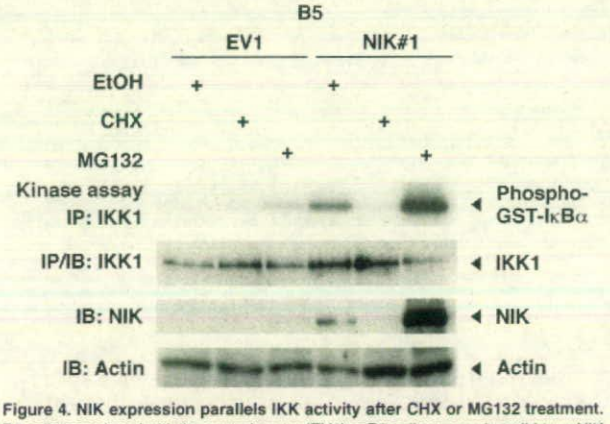

Figure 4. NIK expression parallels IKK activity after CHX or MG132 treatment. B5 cells transduced with the control vector (EV1) or B5 cells expressing wild-type NIK (NIK#1) were treated for 4 hours with either vehicle (ethanol, EtOH), cycloheximide (CHX; 50 μg/mL), or MG132 (20 μM). Cytoplasmic extracts were subjected to immunoprecipitation with IKK1-specific antibody, and then immunoprecipitates were used for an in vitro kinase assay. IKK1 expression in the immunoprecipitates was revealed by immunoblotting with IKK1-specific antibody. NIK and actin levels in the cytoplasmic extracts used for immunoprecipitation were determined by immunoblotting with anti-NIK or antiactin antibodies, respectively. IB indicates immunoblotting; IP, immunoprecipitation; GST, glutathione-S-transferase tag.

We have previously demonstrated that the treatment of ATL cells with MG132 greatly enhances IKK activity, whereas protein synthesis inhibition quickly abolished this activity.[11] Figure 4 shows that the IKK activity in B5 cells stably expressing NIK (NIK#1) is modulated by MG132 and cycloheximide (CHX) in a manner that is very similar to that seen in ATL cells. In addition, treatment of NIK#1 cells with MG132 remarkably elevates the level of exogenous NIK expression. The constitutive NF-κB activation caused by the presence of exogenous NIK was found to be abolished by the retroviral expression of a super-repressor form of IκBα (SR-IκBα), without affecting exogenous NIK expression (Figure 5A). Interestingly, the forced expression of SR-IκBα also diminishes the p52 and p100 expression levels.

We next tested the ability of NIK to induce anchorage-independent growth of rat fibroblasts. B5 and h12 cells transduced with the control vector did not form colonies of significant size in soft agar, whereas those transduced with wild-type NIK expression vector formed a number of large colonies, as shown in Figure 5B and Table 1. Cells expressing catalytically inactive NIK failed to form colonies in soft agar. The expression of SR-IκBα completely abolished NIK-induced colony formation and also the morphologic alterations of B5 and h12 cells. Given that SR-IκBα specifically suppresses NF-κB activation,

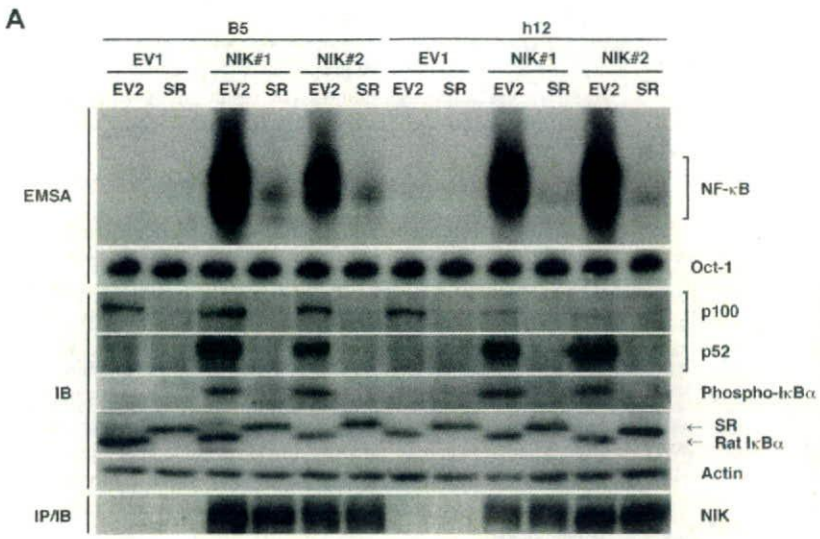

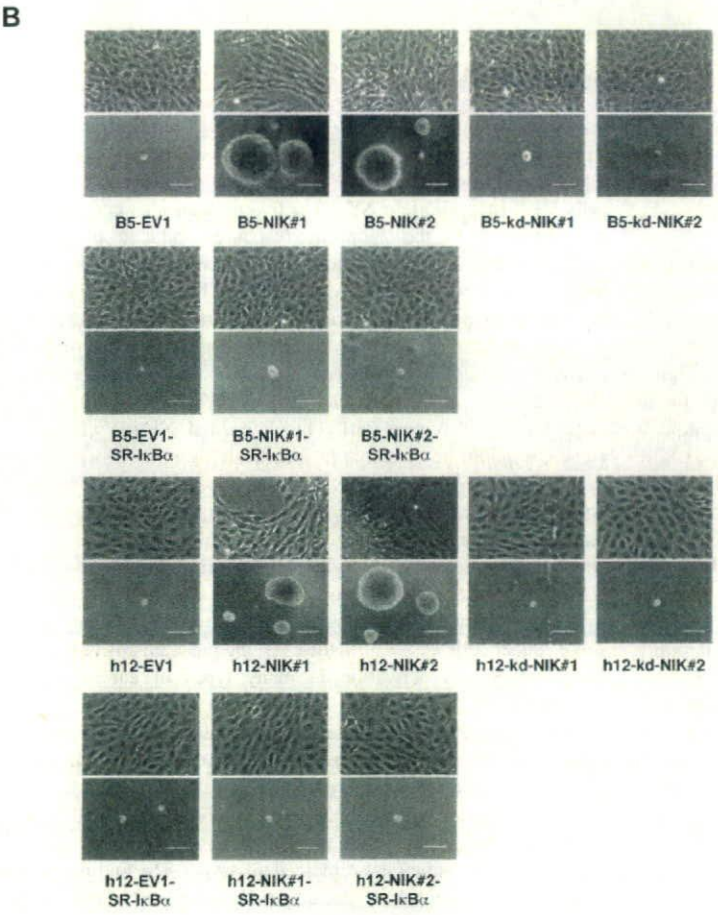

Figure 5. The overexpression of NIK transforms rat fibroblasts in an NF-κB–dependent manner. (A) Top 2 panels: 5 μg of nuclear extracts prepared from B5 and h12 cells transduced with empty vector (EV2) or SR-IκBα (SR) were analyzed by EMSA, using NF-κB and Oct-1 probes. Middle 5 panels: whole-cell extracts (30 μg) of B5 or h12 infectants were subjected to SDS-PAGE and immunoblotting with anti-p52, antiphospho-IκBα, anti-IκBα, or antiactin antibodies. Bottom panel: HA-tagged NIK was immunoprecipitated from B5 and h12 infectants with anti-HA antibody and detected by immunoblotting with anti-NIK antibody (H-248). (B) Phase-contrast micrographs of cells cultured on monolayers (top images) or in soft agar (bottom images). B5 or h12 cell clones expressing wild-type NIK (NIK#1 and NIK#2) or not (EV1) were cultured in soft agar for 3 weeks. These cells were further transduced with SR-IκBα, and then pooled cells were assayed for anchorage-independent growth in soft agar. B5 and h12 cell clones expressing kd-NIK were also examined. Original magnification ×100. Scale bar represents 100 μm. SR indicates super-repressor; kd-NIK, catalytically inactive NIK; IB, immunoblotting; IP, immunoprecipitation.

we conclude from these results that NIK transforms rat fibroblasts in an NF-κB–dependent manner.

NIK mediates constitutive NF-κB activation in ATL cells

The similar modulation of IKK activity by CHX or MG132 in both ATL and B5 cells expressing NIK (Figure 4) suggests that NIK plays an important role in constitutive NF-κB activation in ATL cells. We therefore examined whether the RNA interference-mediated silencing of endogenous *NIK* gene expression would lower NF-κB–dependent transcription in these cells. ED-40515(−) and ATL-43Tb(−) cells were infected with lentiviral constructs that express short hairpin RNA (shRNA) molecules that target mRNA for either *Renilla luciferase* (Ctli) or *NIK* (NIKi), and then subjected to puromycin selection for 2 days. To

Table 1. Efficiency of colony formation in soft agar

Cells*	Colony-forming efficiency, %	Average size of colonies, μm†
B5-EV1	0.7 ± 0.5	62.6 ± 1.5
B5-NIK#1	23.2 ± 2.0‡	236.2 ± 12.6‡
B5-NIK#2	18.9 ± 2.4‡	184.1 ± 19.8‡
B5-kd-NIK#1	1.5 ± 0.3	63.1 ± 1.4
B5-kd-NIK#2	1.3 ± 0.1	62.8 ± 1.8
h12-EV1	1.2 ± 0.3	60.5 ± 0.0
h12-NIK#1	12.8 ± 1.7‡	146.9 ± 4.6‡
h12-NIK#2	17.7 ± 1.7‡	154.9 ± 5.6‡
h12-kd-NIK#1	1.4 ± 1.0	61.5 ± 2.1
h12-kd-NIK#2	1.5 ± 0.4	62.5 ± 4.7
B5-EV1-EV2	1.2 ± 0.3	61.8 ± 1.1
B5-NIK#1-EV2	21.1 ± 1.0‡	193.8 ± 3.7‡
B5-NIK#2-EV2	14.3 ± 1.0‡	150.4 ± 8.7‡
h12-EV1-EV2	1.5 ± 0.7	60.8 ± 0.4
h12-NIK#1-EV2	12.3 ± 1.7‡	119.4 ± 5.6‡
h12-NIK#2-EV2	14.0 ± 1.8‡	160.3 ± 7.2‡
B5-EV1-SR-IκBα	1.5 ± 0.0	61.7 ± 0.5
B5-NIK#1-SR-IκBα	3.4 ± 0.0	64.8 ± 1.1
B5-NIK#2-SR-IκBα	3.9 ± 0.1	63.3 ± 0.4
h12-EV1-SR-IκBα	1.7 ± 1.0	61.3 ± 0.4
h12-NIK#1-SR-IκBα	2.7 ± 0.3	62.3 ± 0.1
h12-NIK#2-SR-IκBα	3.4 ± 1.4	61.4 ± 0.2

kd-NIK indicates catalytically inactive NIK; SR, super-repressor; EV1, empty vector for NIK or kd-NIK; and EV2, empty vector for SR-IκBα.

*Cells were inoculated in 0.33% soft agar and cultured for 3 weeks.

†Colonies larger than 60 μm were counted as positive. The sizes of more than 100 positive colonies were averaged.

‡$P < .05$ vs B5-EV1.

suppress NIK expression maximally, we used independently or in combination 2 shRNAs (NIKi-1 and -2) that target different *NIK* sequences and reduce NIK expression. The infected cells were then assayed for transcriptional activity by transient transfection with an NF-κB–dependent reporter gene (Figure 6A). Lentiviral expression of NIKi constructs resulted in suppression of NF-κB–dependent reporter gene expression in ATL cells when independently used, and the combined use of the 2 NIKi constructs (NIKi-1 and -2) was found to be more effective. We then examined ATL cells transduced with NIKi-1 and -2 constructs for the expression of endogenous NIK and specifically phosphorylated forms of p100, IκBα, and IKKs by immunoblotting (Figure 6B) and for NF-κB DNA binding activity by EMSA (Figure 6C). NIK expression in ATL cells was found to be down-regulated by the shRNA-mediated silencing (Figure 6B). As expected, p52 and phosphorylated p100 were also reduced by NIK depletion, and interestingly, phoshorylation of IκBα was also suppressed. This is consistent with the results observed in NIK-transduced rat fibroblasts that express the phoshorylated form of IκBα (Figure 5A), indicating that NIK, when aberrantly and stably expressed, induces phosphorylation of IκBα. In addition, NIK depletion suppressed phosphorylation of the serine residues in the activation loop of IKKs, suggesting a key role for NIK in constitutive activation of IKKs in ATL cells (Figure 6B). Moreover, depletion of NIK resulted in suppression of NF-κB DNA binding activity (Figure 6C). Super-shift assays revealed that DNA-binding of NF-κB components, p50, p52, RelA, and RelB was reduced by NIK depletion (Figure 6D). As shown previously, c-Rel was not detected in ATL cells.[34] We further investigated alterations in the expression of NF-κB target genes by NIK depletion. Vascular endothelial growth factor (VEGF), matrix metalloproteinase-9 (MMP-9), and intracellular adhesion molecule-1 (ICAM-1), the expression of which has been reported to be under the control of NF-κB,[35-37] are highly expressed in ATL cells and suggested to contribute to their invasive properties.[38-41] Quantitative RT-PCR studies reveal that depletion of NIK results in down-regulation of the expression of these NF-κB target genes (Figure 6E).

NIK regulates tumorigenicity of ATL cells in vivo

We finally investigated biologic effects of NIK depletion in ATL cells. NIK depletion did not significantly influence the growth of cells in culture (Figure 7A). We then examined whether depletion of NIK affects the tumorigenicity of ATL cells in a mouse model. NOD/SCID/γc^{null} mice were subcutaneously inoculated with ED-40515(−) cells that express Ctli or NIKi and are characterized in Figure 6B,C, and tumor formation was evaluated 2 weeks later. As expected, ED-40515(−) cells expressing Ctli efficiently formed large tumors, whereas tumors formed in mice inoculated with ED-40515(−) cells expressing NIKi were significantly smaller (Figure 7B-D), suggesting that NIK supports efficient tumor cell growth in vivo.

Discussion

Persistent activation of NF-κB has previously been reported to play an essential role in the growth and survival of specific cancer cell types, including ATL, H-RS, melanoma, and prostate cancer cells.[9,42-45] Inappropriate NF-κB activation can also contribute to the resistance to the apoptotic responses induced by certain anticancer drugs.[46] On the other hand, cancer cell apoptosis can be induced when persistent NF-κB activity is blocked by inhibitors, such as SR-IκBα, by drugs targeting IKK or the proteasome, via peptides targeting p50 or NEMO, and by double-stranded oligonucleotides containing NF-κB binding sites.[47,48] One problem with such inhibitors, however, is their lack of specificity to cancer cells because they also necessarily block normal NF-κB activation. Hence, it would be desirable to specifically inhibit NF-κB activation in cancer cells by identifying molecular targets in each cancer type. Virally transformed cancer cells express a virus-derived regulatory protein(s) that targets critical molecules in a variety of key signaling pathways. Cytokine autocrine loops or genetic alterations to genes regulating the NF-κB signaling mechanisms that lead to persistent NF-κB activation have also been identified in some cancer cells.[16,17,32,47,49] However, the mechanisms underlying persistent NF-κB activation in many types of cancer remain unknown.

Most primary ATL cells, although infected with HTLV-I, are characterized by the loss of viral protein expression, including Tax, probably because of the host immune surveillance during the long period of latency.[50] Nevertheless, NF-κB is strongly and persistently activated in ATL cells through IKK,[9] although the mechanism of IKK activation has remained unknown. The findings in our present study demonstrate the aberrant expression of *NIK* at the pretranslational level in ATL cells derived from 15 of 21 patients. This overexpression does not seem to correlate with the patients' age, sex, disease type, or percentage of abnormal lymphocytes (Table S1). Further studies will be required to clarify potentially NIK-independent NF-κB activation in the other 6 cases. The stable expression of functional NIK in fibroblasts, but not that of its catalytically inactive mutant, causes cellular transformation and persistent NF-κB activation with molecular features quite similar to those reported previously in ATL cells. These include the rapid

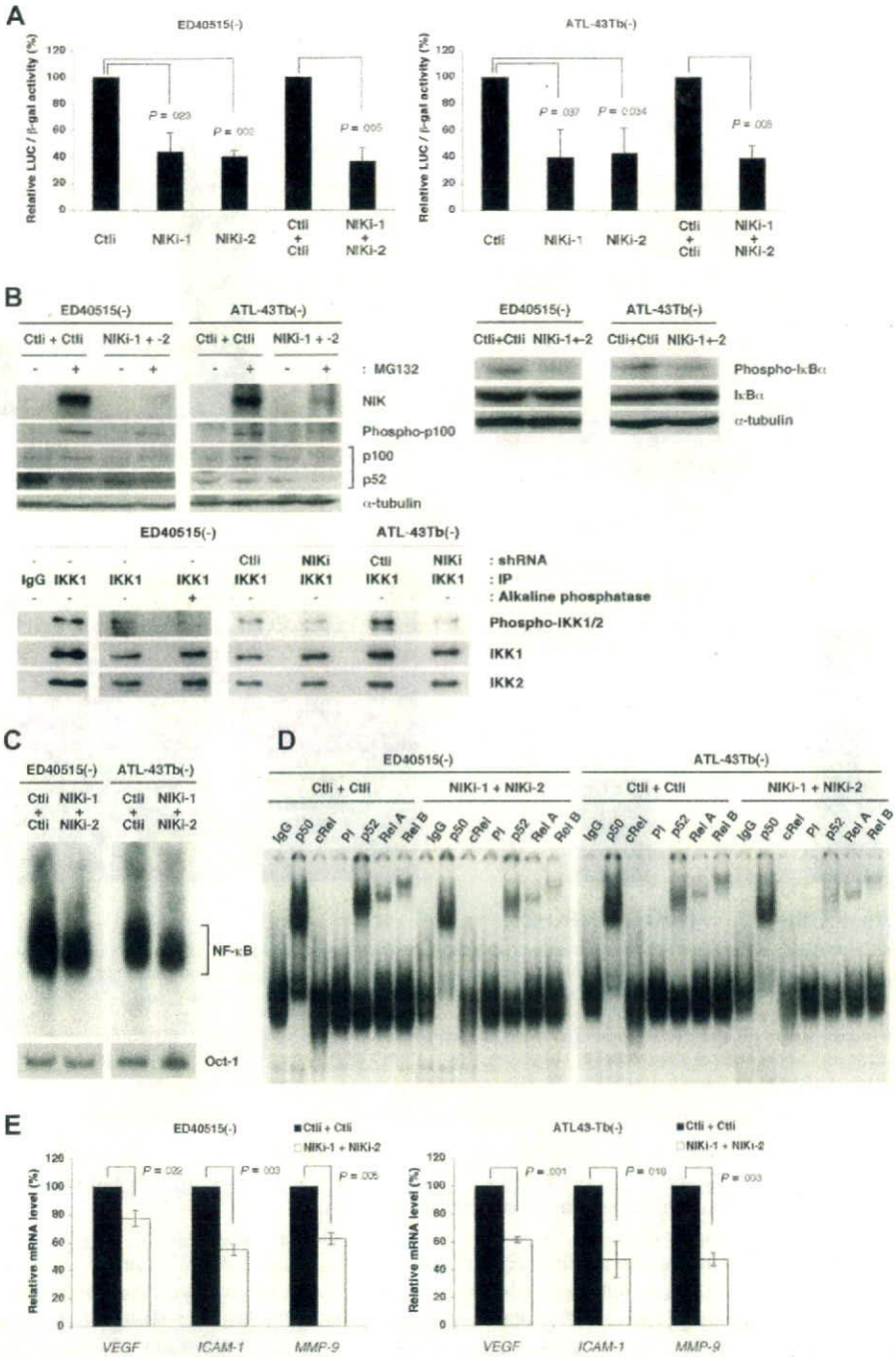

Figure 6. Depletion of NIK suppresses NF-κB-dependent transcription in ATL cells. (A) ED40515(−) and ATL-43Tb(−) cells were infected with lentiviral vectors expressing *Renilla luciferase* (Ctli) or *NIK*-specific shRNAs (NIKi-1 or NIKi-2). In parallel, ED40515(−) and ATL-43Tb(−) cells were infected with lentiviral vectors expressing Ctli or NIKi-1 shRNAs, and 24 hours later, these cells were super-infected with lentiviral vectors expressing Ctli or NIKi-2 shRNAs. Twenty-four hours after infection, cells were selected with puromycin for 2 days. Puromycin-resistant cells were then transfected with 2 μg of IgκCona-Luc and 2 μg EF1-LacZ. Luciferase (LUC) activity was determined 48 hours after transfection and normalized to β-gal activity. Relative luciferase activities, in comparison with control cells, 100 are shown. Data are expressed as mean plus or minus SD of 3 independent experiments. *P* values are versus control (Ctli). (B) Super-infected cells were treated with or without MG132 (20 μM) for 3 hours and subjected to SDS-PAGE and immunoblotting with anti-NIK (#4994), antiphosphorylated p100, or anti-α-tubulin antibodies. Whole-cell extracts (30 μg) from these cells were analyzed by SDS-PAGE and immunoblotting with antiphospho-IκBα, anti-IκBα, or anti-α-tubulin antibodies. Cytoplasmic extracts prepared from ED40515(−) cells infected or not with lentivirus were precleared and immunoprecipitation was performed, using anti-IKK1 monolconal antibody or its isotype IgG (IgG). After 3 washes with TNT buffer, immune complexes were treated or not with Shrimp Akaline Phosphatase (Takara Bio) and then subjected to SDS-PAGE and immunoblotting with antiphospho-IKK1/2, anti-IKK1, or anti-IKK2 antibodies. (C) A total of 5 μg of nuclear extracts prepared from lentivirus-infected cells shown in panel B were analyzed by EMSA, using oligonucleotides encoding the NF-κB–binding sequence or Oct-1–binding sequence as probes. (D) Nuclear extracts (5 μg) from lentivirus-infected cells shown in panel B were preincubated for 30 minutes with purified mouse IgG, anti-p50, anti-cRel antibody, preimmune (PI), anti-p50, anti-RelA or anti-RelB sera, and then subjected to EMSA with the NF-κB–specific probe. (E) Total RNAs from lentivirus-infected cells shown in panel B were examined by quantitative RT-PCR for *VEGF*, *ICAM-1*, and *MMP-9* mRNA levels. Each mRNA level was normalized to *18S* RNA. Relative mRNA levels, in comparison with control cells, 100 are shown. Data are expressed as mean plus or minus SD of 3 independent experiments. *P* values are versus control (Ctli + Ctli).

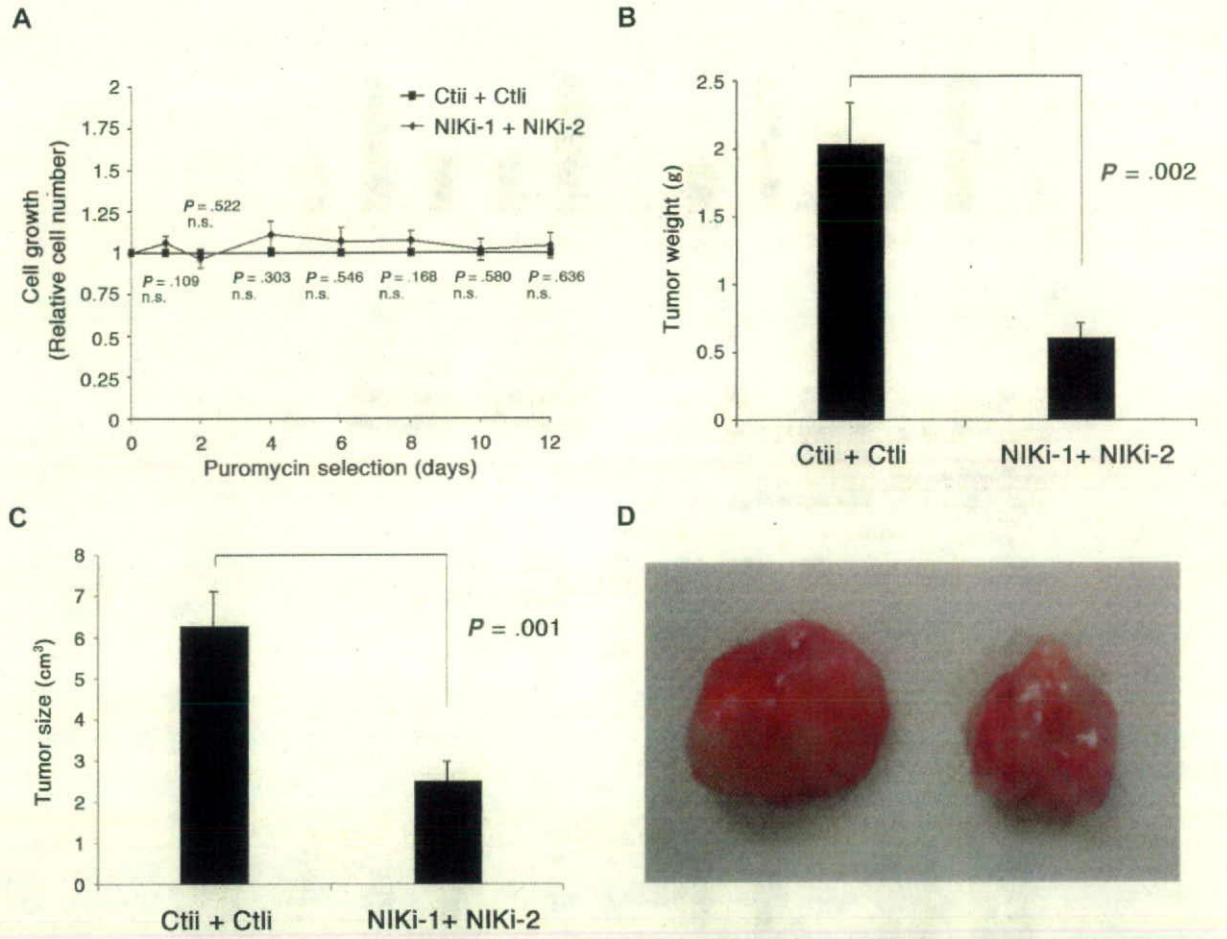

Figure 7. Depletion of NIK in ATL cells suppresses tumor formation in NOD-SCID/γc^{null} (NOG) mice. (A) Pools of ED40515(−) cells expressing Ctli or NIKi-1 and -2, shown in Figure 6B, C, D, and E, were analyzed for cell growth in vitro by the trypan blue staining method. Relative cell numbers, in comparison with control cells (arbitrarily set at 1), are shown. Data are expressed as mean plus or minus SD of 3 independent experiments. *P* values are vs control (Ctli + Ctli). n.s. indicates no significant difference. (B-D) NOG mice were inoculated subcutaneously in the postauricular region with the puromycin-resistant ED-40515(−) cells (5×10^6). Tumor formation in mice was evaluated 2 weeks after inoculation. Tumor weight (B) and size (C) relative to those of tumors formed in mice inoculated with ED40515(−) cells expressing Ctli are shown. (D) Photographs of tumors formed 2 weeks after cell inoculation. Each result was obtained from 5 different mice (means are shown [error bars]). *P* values are versus control (Ctli + Ctli).

loss of IKK activity after protein synthesis inhibition and the superinduction of IKK activity in the presence of MG132.[11] Moreover, RNA interference studies have also indicated that the deregulated NIK expression is the principal cause of constitutive NF-κB activation in ATL cells. In line with a previous report by Ramakrishnan et al, which showed that the induction of IκBα degradation by CD70, CD40 ligand, and BLyS/BAFF is dependent on the function of NIK,[18] we find in our present experiments that the stable expression of NIK induces IκBα phosphorylation and the formation of DNA binding complexes containing not only p50 and RelB, but also RelA both in wild-type and in NEMO-deficient rat fibroblasts. This indicates that NIK can stimulate the canonical pathway characterized by IκBα phosphorylation and RelA activation and that NIK does not require NEMO for it. Interestingly, the forced expression of SR-IκBα in these fibroblasts abolishes the transformed phenotype and suppresses constitutive NF-κB activity, with the p100 and p52 expression levels being diminished simultaneously, probably because p100 expression is largely dependent on NF-κB activity.[51] RelB expression is also known to be controlled by NF-κB,[52] suggesting that the noncanonical pathway of NF-κB activation does not work independently but rather coincides with NF-κB activation through the canonical pathway under stable conditions.

H-RS cells were also found to overexpress NIK, including its transcripts, in this study. Earlier reports have described 2 potential mechanisms of constitutive NF-κB activation in H-RS cells: persistent signaling from receptors that cause NF-κB activation, such as CD30, CD40, and RANK as well as a CD40-like molecule latent membrane protein 1 of the Epstein-Barr virus; and disruption of IκBα-dependent suppression resulting from the mutation of this gene.[32,48] The H-RS cell lines used in this study are Epstein-Barr virus-negative, and neither HDLM-2 nor L540 cells harbor mutations in their *IκB* genes. Indeed, CD30, CD40, and RANK were all found to be expressed in the H-RS cell lines used in this study, but we envisage that the aberrant expression of NIK is a distinct mechanism underlying the persistent NF-κB activation in these cells. It is partly because these TNF family receptor molecules, when stimulated or overexpressed transiently in cultured cells, elevate the NIK protein expression levels with a concomitant reduction in TRAF3 but do not increase *NIK* mRNA.[19,20]

Whereas the transient stimulation of a B-cell line with BAFF or anti-CD40 antibody stabilizes the NIK protein at the posttranslational level and does not up-regulate its mRNA expression,[20] NIK was observed to be constitutively overexpressed in ATL and H-RS cells at the pretranslational level. These differing mechanisms of NIK regulation may not be all that surprising, however, in light of the transient vs persistent nature of the activation of NF-κB. The barely detectable levels of steady-state NIK protein expression and its robust accumulation after proteasome inhibition in ATL and H-RS cells further suggest that the proteasome-dependent degradation of NIK occurs rapidly in tumor cells as in normal cells, although we cannot rule out the possibility that TNF family receptors known to be overexpressed in H-RS cells influence the stability of NIK to some extent. This point is currently very difficult to address because the protein amount of NIK in the absence of the proteasome inhibitor is quite limited. At least 3 mechanisms of pretranslational induction of NIK are plausible: the stabilization of *NIK* transcripts, transcriptional activation and/or amplification of the *NIK* gene. It should be noted that the stability of *NIK* mRNA in ATL cells was similar to that in control cells, suggesting that NIK expression is deregulated in ATL cells at the level of mRNA production. In this regard, we are currently analyzing the regulatory region of the *NIK* gene in normal and cancer cells.

We detected NIK in whole-cell lysates only when the cells themselves were treated with the proteasome inhibitor, MG132. It is possible that the expression of the NIK protein is tightly regulated under detectable levels in resting normal cells. However, in ATL and H-RS cells, enhanced NIK production, although still not detectable by simple immunoblotting, may be sufficient to cause its deregulated activity toward IKK. During the manuscript preparation, 2 reports demonstrated deregulated expression of NIK because of mutations in *TRAF3, CYLD*, or *NIK* itself in multiple myeloma cells.[16,17] In case of ATL cells, formation of a fusion protein after genomic rearrangement seems to be unlikely based on the apparently normal size of the protein. At present, the mechanism of overproduction of *NIK* mRNA in ATL cells remains to be determined, but the fluorescence in situ hybridization results suggest that aberrant NIK expression in ATL cells is not the result of genomic abnormalities, such as amplification or translocation.

Successful anticancer drug or gene therapies can be conducted in a number of ways, including the general administration of particular reagents that mechanistically work exclusively on cancer cells, or delivering conventional anticancer reagents specifically to cancer cells. The former strategy is likely to be more promising in the case of hematopoietic cancers. In this regard, NIK could be an attractive molecular target for ATL and Hodgkin lymphoma therapy, although the physiologic functions of NIK in human adults remain unknown. Suppressing high NF-κB activity levels by targeting NIK may also sensitize these cancer cells to commonly used anticancer agents.

Acknowledgments

The authors thank all of the ATL patients who donated blood samples for use in this study, Dr K. Yamaguchi and the Joint Study on Predisposing Factors of ATL Development for providing and analyzing sample blood, and the following researchers for donating invaluable reagents: Dr M. Maeda (Kyoto University, Kyoto, Japan) for the ED40515(−) and ATL-43Tb(−) cells, Dr D. Goeddel (Amgen, Thousand Oaks, CA) for *NIK* cDNAs, Dr N.R. Rice and Dr A. Israël (Institut Pasteur Paris, Paris, France) for p50, RelA, and RelB antisera, Dr T. Kitamura (University of Tokyo, Tokyo, Japan) for Plat-E cells, Dr I.S.Y. Chen (UCLA, Los Angeles, CA) for pHCMV-VSVG and pCMVΔR8.2 packaging plasmids, and Dr H. Miyoshi (RIKEN Tsukuba Institute, Tsukuba, Japan) for CS-CDF-CG-PRE plasmid. The authors also thank Dr G. Courtois (INSERM, Paris, France) and the members of the Department of Molecular Virology for helpful discussions.

This work was supported by research grants from the Ministry of Health and Labor Sciences (HIV/AIDS, H18-005) (Naoki Yamamoto) and from the Ministry of Education, Culture, Sports, Science and Technology of Japan (18390145; Naoki Yamamoto) and (17013029; S.Y.).

Authorship

Contribution: Y.S., T.S., and S.Y. designed the study; Y.S., Norio Yamamoto, H.S., V.J.M.B., Y.I., K.M., X.Q., I.I., J.I., and S.Y. carried out the research; M.Z.D. carried out the animal experiments; A.U. and T.W. collected and analyzed sample blood from ATL patients; T.M. contributed to lentiviral vector constructions; Y.S. and S.Y. analyzed the data; T.S., Naoki Yamamoto and S.Y. controlled the data; Y.S. and S.Y. wrote the paper; all authors checked the final version of the manuscript.

Conflict-of-interest disclosure: The authors declare no competing financial interests.

Correspondence: Shoji Yamaoka, Department of Molecular Virology, Graduate School of Medicine, Tokyo Medical and Dental University, 1-5-45, Yushima, Bunkyo-ku, Tokyo, 113-8510, Japan; e-mail: shojmmb@tmd.ac.jp.

References

1. Baldwin AS Jr. Series introduction: the transcription factor NF-kappaB and human disease. J Clin Invest. 2001;107:3-6.
2. Hayden MS, Ghosh S. Signaling to NF-kappaB. Genes Dev. 2004;18:2195-2224.
3. Xiao G, Rabson AB, Young W, Qing G, Qu Z. Alternative pathways of NF-kappaB activation: a double-edged sword in health and disease. Cytokine Growth Factor Rev. 2006;17:281-293.
4. Coope HJ, Atkinson PG, Huhse B, et al. CD40 regulates the processing of NF-kappaB2 p100 to p52. EMBO J. 2002;21:5375-5385.
5. Claudio E, Brown K, Park S, Wang H, Siebenlist U. BAFF-induced NEMO-independent processing of NF-kappa B2 in maturing B cells. Nat Immunol. 2002;3:958-965.
6. Karin M, Cao Y, Greten FR, Li ZW. NF-kappaB in cancer: from innocent bystander to major culprit. Nat Rev Cancer. 2002;2:301-310.
7. Jost PJ, Ruland J. Aberrant NF-{kappa}B signaling in lymphoma: mechanisms, consequences and therapeutic implications. Blood. 2006;109:2700-2707.
8. Ni H, Ergin M, Huang Q, et al. Analysis of expression of nuclear factor kappa B (NF-kappa B) in multiple myeloma: downregulation of NF-kappa B induces apoptosis. Br J Haematol. 2001;115:279-286.
9. Hironaka N, Mochida K, Mori N, Maeda M, Yamamoto N, Yamaoka S. Tax-independent constitutive IkappaB kinase activation in adult T-cell leukemia cells. Neoplasia. 2004;6:266-278.
10. Nonaka M, Horie R, Itoh K, Watanabe T, Yamamoto N, Yamaoka S. Aberrant NF-kappaB2/p52 expression in Hodgkin/Reed-Sternberg cells and CD30-transformed rat fibroblasts. Oncogene. 2005;24:3976-3986.
11. Miura H, Maeda M, Yamamoto N, Yamaoka S. Distinct IkappaB kinase regulation in adult T cell leukemia and HTLV-I-transformed cells. Exp Cell Res. 2005;308:29-40.
12. Dejardin E, Bonizzi G, Bellahcene A, Castronovo V, Merville MP, Bours V. Highly-expressed p100/p52 (NFKB2) sequesters other NF-kappa B-related proteins in the cytoplasm of human breast cancer cells. Oncogene. 1995;11:1835-1841.
13. Lessard L, Begin LR, Gleave ME, Mes-Masson AM, Saad F. Nuclear localization of nuclear factor-kappaB transcription factors in prostate cancer: an immunohistochemical study. Br J Cancer. 2005;93:1019-1023.
14. Chandler NM, Canete JJ, Callery MP. Increased

expression of NF-kappa B subunits in human pancreatic cancer cells. J Surg Res. 2004;118:9-14.

15. Bours V, Dejardin E, Goujon-Letawe F, Merville MP, Castronovo V. The NF-kappa B transcription factor and cancer: high expression of NF-kappa B- and I kappa B-related proteins in tumor cell lines. Biochem Pharmacol. 1994;47:145-149.
16. Annunziata CM, Davis RE, Demchenko Y, et al. Frequent engagement of the classical and alternative NF-kappaB pathways by diverse genetic abnormalities in multiple myeloma. Cancer Cell. 2007;12:115-130.
17. Keats JJ, Fonseca R, Chesi M, et al. Promiscuous mutations activate the noncanonical NF-kappaB pathway in multiple myeloma. Cancer Cell. 2007;12:131-144.
18. Ramakrishnan P, Wang W, Wallach D. Receptor-specific signaling for both the alternative and the canonical NF-kappaB activation pathways by NF-kappaB-inducing kinase. Immunity. 2004;21:477-489.
19. Liao G, Zhang M, Harhaj EW, Sun SC. Regulation of the NF-kappaB-inducing kinase by tumor necrosis factor receptor-associated factor 3-induced degradation. J Biol Chem. 2004;279:26243-26250.
20. Qing G, Qu Z, Xiao G. Stabilization of basally translated NF-kappaB-inducing kinase (NIK) protein functions as a molecular switch of processing of NF-kappaB2 p100. J Biol Chem. 2005;280:40578-40582.
21. Maeda M, Shimizu A, Ikuta K, et al. Origin of human T-lymphotrophic virus I-positive T cell lines in adult T cell leukemia: analysis of T cell receptor gene rearrangement. J Exp Med. 1985;162:2169-2174.
22. Yagi H, Nomura T, Nakamura K, et al. Crucial role of FOXP3 in the development and function of human CD25$^+$CD4$^+$ regulatory T cells. Int Immunol. 2004;16:1643-1656.
23. Sugamura K, Fujii M, Kannagi M, Sakitani M, Takeuchi M, Hinuma Y. Cell surface phenotypes and expression of viral antigens of various human cell lines carrying human T-cell leukemia virus. Int J Cancer. 1984;34:221-228.
24. Foley GE, Lazarus H, Farber S, Uzman BG, Boone BG, McCarthy RE. Continuous cultured human lymphoblasts from peripheral blood of a child with acute leukemia. Cancer. 1965;18:522-529.
25. Weiss A, Wiskocil RL, Stobo JD. The role of T3 surface molecules in the activation of human T cells: a two-stimulus requirement for IL 2 production reflects events occurring at pre-translational level. J Immunol. 1984;133:123-128.
26. Yamaoka S, Courtois G, Bessia C, et al. Complementation cloning of NEMO, a component of the IkappaB kinase complex essential for NF-kappaB activation. Cell. 1998;93:1231-1240.
27. Chinanonwait N, Miura H, Yamamoto N, Yamaoka S. A recessive mutant cell line with a constitutive IkappaB kinase activity. FEBS Lett. 2002;531:553-560.
28. Morita S, Kojima T, Kitamura T. Plat-E: an efficient and stable system for transient packaging of retroviruses. Gene Ther. 2000;7:1063-1066.
29. Yamaoka S, Inoue H, Sakurai M, et al. Constitutive activation of NF-kappa B is essential for transformation of rat fibroblasts by the human T-cell leukemia virus type I Tax protein. EMBO J. 1996;15:873-887.
30. Munoz E, Courtois G, Veschambre P, Jalinot P, Israël A. Tax induces nuclear translocation of NF-kappa B through dissociation of cytoplasmic complexes containing p105 or p100 but does not induce degradation of I kappa B alpha/MAD3. J Virol. 1994;68:8035-8044.
31. Dewan MZ, Terashima K, Taruishi M, et al. Rapid tumor formation of human T-cell leukemia virus type 1-infected cell lines in novel NOD-SCID/γc^{null} mice: suppression by an inhibitor against NF-κB. J Virol. 2003;77:5286-5294.
32. Krappmann D, Emmerich F, Kordes U, Scharschmidt E, Dorken B, Scheidereit C. Molecular mechanisms of constitutive NF-kappaB/Rel activation in Hodgkin/Reed-Sternberg cells. Oncogene. 1999;18:943-953.
33. Wood KM, Roff M, Hay RT. Defective IkappaBalpha in Hodgkin cell lines with constitutively active NF-kappaB. Oncogene. 1998;16:2131-2139.
34. Mori N, Fujii M, Ikeda S, et al. Constitutive activation of NF-kappaB in primary adult T-cell leukemia cells. Blood. 1999;93:2360-2368.
35. Yemelyanov A, Gasparian A, Lindholm P, et al. Effects of IKK inhibitor PS1145 on NF-kappaB function, proliferation, apoptosis and invasion activity in prostate carcinoma cells. Oncogene. 2006;25:387-398.
36. Farina AR, Tacconelli A, Vacca A, Maroder M, Gulino A, Mackay AR. Transcriptional up-regulation of matrix metalloproteinase-9 expression during spontaneous epithelial to neuroblast phenotype conversion by SK-N-SH neuroblastoma cells, involved in enhanced invasivity, depends upon GT-box and nuclear factor kappaB elements. Cell Growth Differ. 1999;10:353-367.
37. Collins T, Read MA, Neish AS, Whitley MZ, Thanos D, Maniatis T. Transcriptional regulation of endothelial cell adhesion molecules: NF-kappa B and cytokine-inducible enhancers. FASEB J. 1995;9:899-909.
38. El-Sabban ME, Merhi RA, Haidar HA, et al. Human T-cell lymphotropic virus type 1-transformed cells induce angiogenesis and establish functional gap junctions with endothelial cells. Blood. 2002;99:3383-3389.
39. Mori N, Sato H, Hayashibara T, et al. Human T-cell leukemia virus type I Tax transactivates the matrix metalloproteinase-9 gene: potential role in mediating adult T-cell leukemia invasiveness. Blood. 2002;99:1341-1349.
40. Hayashibara T, Yamada Y, Onimaru Y, et al. Matrix metalloproteinase-9 and vascular endothelial growth factor: a possible link in adult T-cell leukaemia cell invasion. Br J Haematol. 2002;116:94-102.
41. Fukudome K, Furuse M, Fukuhara N, Orita T, Hinuma Y. Strong induction of ICAM-1 in human T cells transformed by human T-cell leukemia virus type 1 and depression of ICAM-1 or LFA-1 in adult T-cell leukemia-derived cell lines. Int J Cancer. 1992;52:418-427.
42. Mori N, Yamada Y, Ikeda S, et al. Bay 11–7082 inhibits transcription factor NF-kappaB and induces apoptosis of HTLV-I-infected T-cell lines and primary adult T-cell leukemia cells. Blood. 2002;100:1828-1834.
43. Bargou RC, Emmerich F, Krappmann D, et al. Constitutive nuclear factor-kappaB-RelA activation is required for proliferation and survival of Hodgkin's disease tumor cells. J Clin Invest. 1997;100:2961-2969.
44. Yang J, Amiri KI, Burke JR, Schmid JA, Richmond A. BMS-345541 targets inhibitor of kappaB kinase and induces apoptosis in melanoma: involvement of nuclear factor kappaB and mitochondria pathways. Clin Cancer Res. 2006;12:950-960.
45. Gasparian AV, Yao YJ, Kowalczyk D, et al. The role of IKK in constitutive activation of NF-kappaB transcription factor in prostate carcinoma cells. J Cell Sci. 2002;115:141-151.
46. Wang CY, Cusack JC Jr, Liu R, Baldwin AS Jr. Control of inducible chemoresistance: enhanced anti-tumor therapy through increased apoptosis by inhibition of NF-kappaB. Nat Med. 1999;5:412-417.
47. Gilmore TD, Herscovitch M. Inhibitors of NF-kappaB signaling: 785 and counting. Oncogene. 2006;25:6887-6899.
48. Braun T, Carvalho G, Fabre C, Grosjean J, Fenaux P, Kroemer G. Targeting NF-kappaB in hematologic malignancies. Cell Death Differ. 2006;13:748-758.
49. Courtois G, Gilmore TD. Mutations in the NF-kappaB signaling pathway: implications for human disease. Oncogene. 2006;25:6831-6843.
50. Sun SC, Yamaoka S. Activation of NF-kappaB by HTLV-I and implications for cell transformation. Oncogene. 2005;24:5952-5964.
51. Liptay S, Schmid RM, Nabel EG, Nabel GJ. Transcriptional regulation of NF-kappa B2: evidence for kappa B-mediated positive and negative autoregulation. Mol Cell Biol. 1994;14:7695-7703.
52. Bren GD, Solan NJ, Miyoshi H, Pennington KN, Pobst LJ, Paya CV. Transcription of the RelB gene is regulated by NF-kappaB. Oncogene. 2001;20:7722-7733.

ELSEVIER

INSTITUT PASTEUR

Microbes and Infection 10 (2008) 748–756

www.elsevier.com/locate/micinf

Original article

Induction of apoptosis in Epstein-Barr virus-infected B-lymphocytes by the NF-κB inhibitor DHMEQ

Ariko Miyake [a,1], Md. Zahidunnabi Dewan [b,c,1], Takaomi Ishida [a], Mariko Watanabe [d], Mitsuo Honda [c], Tetsutaro Sata [e], Naoki Yamamoto [b,c,**], Kazuo Umezawa [f], Toshiki Watanabe [a,***], Ryouichi Horie [d,*]

[a] *Laboratory of Tumor Cell Biology, Department of Medical Genome Sciences, Graduate School of Frontier Sciences, University of Tokyo, 4-6-1 Shirokanedai, Minato-ku, Tokyo 108-8639, Japan*

[b] *Department of Molecular Virology, Bio-Response, Graduate School, Tokyo Medical and Dental University, 1-5-45 Yushima, Bunkyo-ku, Tokyo 113-8519, Japan*

[c] *AIDS Research Center, National Institute of Infectious Diseases, 1-23-1 Toyama, Shinjuku-ku, Tokyo 162-8640, Japan*

[d] *Department of Hematology, School of Medicine, Kitasato University, 1-15-1 Sagamihara, Kanagawa 228-8555, Japan*

[e] *Department of Pathology, National Institute of Infectious Diseases, 1-23-1 Toyama, Shinjuku-ku, Tokyo 162-8640, Japan*

[f] *Department of Applied Chemistry, Faculty of Science and Technology, Keio University, 3-14-1 Hiyoshi, Kohoku-ku, Yokohama, Kanagawa 223-0061, Japan*

Received 19 January 2008; accepted 9 April 2008
Available online 13 April 2008

Abstract

Epstein–Barr virus (EBV) causes EBV-associated lymphoproliferative diseases in patients with profound immune suppression. Most of these diseases are life-threatening and the prognosis of AIDS-associated lymphomas is extremely unfavorable. Polyclonal expansion of virus infected B-cell predisposes them to transformation. We investigated the possibility of nuclear factor kappa B (NF-κB) inhibition by dehydroxymethylepoxyquinomicin (DHMEQ) for the treatment and prevention of EBV-associated lymphoproliferative diseases. We examined the effect of DHMEQ on apoptosis induction in four EBV-transformed lymphoblastoid cell lines as well as peripheral blood mononuclear cells infected with EBV under immunosuppressed condition. DHMEQ inhibits NF-κB activation in EBV-transformed lymphoblastoid cell lines and induces apoptosis by activation of mitochondrial and membranous pathways. Using an *in vivo* NOD/SCIDγc mouse model, we showed that DHMEQ has a potent inhibitory effect on the growth of lymphoblastoid cells. In addition, DHMEQ selectively purges EBV-infected cells expressing latent membrane protein (LMP) 1 from peripheral blood mononuclear cells and inhibits the outgrowth of lymphoblastoid cells. These results suggest that NF-κB is a molecular target for the treatment and prevention of EBV-associated lymphoproliferative diseases. As a potent NF-κB inhibitor, DHMEQ is a potential compound for applying this strategy in clinical medicine.

Keywords: Epstein–Barr virus infections; NF-κB; DHMEQ

1. Introduction

Epstein–Barr virus (EBV) is a member of the γ-herpesvirus family that infects more than 90% of the world population and initially establishes latency III infection in B lymphocytes [1]. Latency III infection is characterized by the expression of the entire array of EBV latency genes, including EBV nuclear proteins (EBNA1, -2, -3A, -3B, -3C, and -LP), integral latent membrane proteins (LMP1, -2A, and -2B), the BamA

* Corresponding author. Tel.: +81 42 778 8111; fax: +81 42 778 8441.
** Tel.: +81 3 5803 5178; fax: +81 3 5803 0124.
*** Tel.: +81 3 5449 5298; fax: +81 3 5449 5418.
E-mail addresses: yamamoto.mmb@tmd.ac.jp (N. Yamamoto), tnabe@ims.u-tokyo.ac.jp (T. Watanabe), rhorie@med.kitasato-u.ac.jp (R. Horie).
[1] These authors contributed equally to this work.

1286-4579/$ - see front matter © 2008 Elsevier Masson SAS. All rights reserved.
doi:10.1016/j.micinf.2008.04.002

rightward transcripts (BARTs), and small RNAs (EBERs). Immune response mediated by T-lymphocytes eliminates most latency III-infected cells; however, resting memory B lymphocytes provide a reservoir for latent virus. T-lymphocyte immunity to latency III-infected B lymphocytes persists for life and protects reactivation of latent virus from a reservoir [2].

However, in the absence of an effective immune response, reactivation of latent virus from a reservoir occurs and causes EBV-associated lymphoproliferative diseases. EBV-associated lymphoproliferative diseases occur with primary infection after transplantation or reactivation of latent virus as a consequence of immune suppression for organ transplantation and autoimmune diseases or acquired immune deficiency syndrome (AIDS) [3–6]. EBV-associated lymphoproliferative diseases are associated in the majority of cases with latency type III phenotype. The prognosis of EBV-associated lymphoproliferative diseases is variable; however, most of these are life-threatening and the prognosis of AIDS-associated lymphomas is extremely unfavorable, although introduction of highly active anti-retroviral treatment (HAART) decreased the incidence, increased the effectiveness of chemotherapy, and improved survival [5]. EBV infection of B-lymphocytes *in vitro* also results in latency III infection and sustained cell proliferation as lymphoblastoid cell lines (LCLs).

Activation of nuclear factor kappa B (NF-κB) has been connected with resistance against apoptosis and tumorigenesis [7]. Despite the diversity in clinical manifestations of EBV-associated lymphoproliferative diseases, strong and constitutive NF-κB activity is reported to be a common characteristic of this disease entity. LMP1 mimics signaling from tumor necrosis factor (TNF) receptor family members by association with tumor necrosis factor receptor-associated factors (TRAFs) and activates the IKK (IκB kinase)−NF-κB pathway [8].

NF-κB represents five cellular proteins: c-Rel, RelA (p65), RelB, NF-κB1 (p50 and its precursor p105), and NF-κB2 (p52 and its precursor p100). The IκB inhibitory proteins consist of IκBα, IκBβ, IκBε, IκBγ, and Bcl-3. NF-κB forms homo- or heterodimers and exists as an inactive complex with IκB regulatory proteins in the cytoplasm. Various signaling pathways converge into IKK-mediated degradation of IκB proteins and subsequent release of uncomplexed NF-κB, which then migrates into the nucleus and activates the transcription of target genes [9].

Dehydroxymethylepoxyquinomicin (DHMEQ) is a new NF-κB inhibitor that is a 5-dehydroxymethyl derivative of the novel compound epoxyquinomicin C that has a 4-hydroxy-5,6-epoxycyclohexenone structure like panepoxydone. Panepoxydone had been found to inhibit TNF-α-induced activation of NF-κB [10]. We have shown that DHMEQ inhibits NF-κB at the level of nuclear translocation [11].

In this study, to investigate the possibility of NF-κB inhibition by DHMEQ as a strategy for the treatment and prevention of EBV-associated lymphoproliferative diseases, we investigated the effect of DHMEQ on apoptosis induction in four EBV-transformed LCLs as well as peripheral blood mononuclear cells (PBMC) in the early phase of EBV infection, and further examined the molecular mechanism of DHMEQ-induced apoptosis.

2. Materials and methods

2.1. Cells

B95.8 EBV-transformed LCLs were established by infection of lymphocytes from four healthy donors with culture supernatants of the virus producer B95.8 line as described previously [12], and are indicated in the text by the first two letters of the name of each donor. In all experiments to test the effects of DHMEQ treatment, LCLs were maintained in RPMI 1640 medium supplemented with 10% fetal bovine serum (FBS).

2.2. Chemicals

DHMEQ is an NF-κB inhibitor that blocks nuclear translocation of NF-κB [11]. DHMEQ was dissolved with dimethylsulfoxide (DMSO). DHMEQ or DMSO was used for experiments at indicated concentrations. Bisbenzimide H 33342 fluorochrome (Hoechst 33342) was purchased from Calbiochem (Bad Soden, Germany).

2.3. Electrophoretic mobility shift analysis

Electrophoretic mobility shift analysis (EMSA) was carried out according to the methods described previously [13]. For detecting NF-κB binding, a double-stranded oligonucleotide containing the κB site of the promoter for the mouse H-2Kb class I major histocompatibility antigen gene was used as a probe [14]. The nucleotide sequence is 5′-GAT CCG GCT GGG AAT CCC CGC TGG GAA TCC CCA TCT A-3′. For control EMSA, a double-strand oligonucleotide containing Oct-1 consensus sequence (Promega, Madison, WI, USA) was used as a probe. Antibodies used for supershift assays were as follows: NF-κB p50 (C-19) goat polyclonal antibody, rabbit polyclonal antibody for NF-κB p65 (C-20) and RelB (C-19), and mouse monoclonal antibody for c-Rel (B-6) and NF-κB p52 (C-5) (all from Santa Cruz Biotechnology Inc., Santa Cruz, CA). A mouse IgG antibody (Sigma, St. Louis, MO) served as a control.

2.4. Cell viability assay

The effects of DHMEQ on cell viability were assayed by color reaction with a tetrazolium salt, WST-8(4-[3-(2-methoxy-4-nitrophenyl)-2-[4-nitrophenyl]-2*H*-5-tetrazolio]-1,3-benzene disulfonate sodium salt) (Cell Counting Kit-8; Dojindo Laboratories, Kumamoto, Japan). After incubation with DHMEQ or DMSO at the indicated concentrations and time points, cells were treated with Cell Counting Kit-8 according to the manufacturer's recommendations and the results were measured by a microplate reader (Bio-Rad, Richmond, CA) at a test wavelength of 450 nm and reference wavelength of 630 nm.